Bunch Shaping in Electron Linear Accelerators

YINE SUN

Advanced Photon Source
Argonne National Lab.

Nov. 7, 2022
20th Advanced Accelerator Concepts Workshop
Long Island, New York

Argonne NATIONAL LABORATORY

Outline

This lecture is based on the article, "Bunch Shaping in Electron Linac Accelerators," by G. Ha, K-J. Kim. P. Piot, J. G. Power and Y. Sun, REVIEWS OF MODERN PHYSICS, VOLUME 94, APRIL–JUNE 2022.
Please refer to the article for links to references and additional information.

- Beam control via electron gun
- Beam control within 1 degree of freedom
- Beam control via phase-space manipulation
  - Round-to-flat Beam Transformation
  - Transverse-to-longitudinal Emittance EXchange (EEX)
  - Longitudinal phase-space shaping via EEX.
  - Double EEX;
  - Round-to-Flat Combined with EEX.
- Summary

Beam Shape Control at the Gun

- Electron gun=Cathode + accelerating/focusing field
- Cathodes with different emission process:
  - Field emitter
    - Great potential; demonstrated transverse shaping; has similar challenges as in thermionic cathode with a large energy spread.
  - Thermionic cathode
    - Robust– workhorse for storage ring light source.
  - Photocathode
    - Linac based light sources
    - Transverse and longitudinal beam shaping
  - Hybrid cathode – photo-assisted field emission or thermionic emission
- Gun
  - DC
  - Rf

Field Emission Cathodes

- Field emitters – small tips are capable of extremely high local current densities (jFE ~ 106 A=mm2) with small emission areas (~100 nm2). Large-area engineered FE cathodes can be based on field emission arrays (FEAs) (Jarvis et al., 2010), carbon nanotubes (CNTs) (Laszczyk, 2020), and ultrananocrystalline diamonds (UNCDs) (Baryshev et al., 2014). All of their surfaces are composed of a quasicontinuous distribution of electron emitters. The distance between the emitters is largest for FEAs(10 μm), smaller for CNTs (0.1–1 μm), and smallest for UNCDs (10–100 nm).
- FEA-based cathodes have been used to generate both continuous (such as triangular) and modulated (such as in an array of beamlets) transverse distributions. However space-charge effects and the long phase emission period are suspected to have blurred the image.

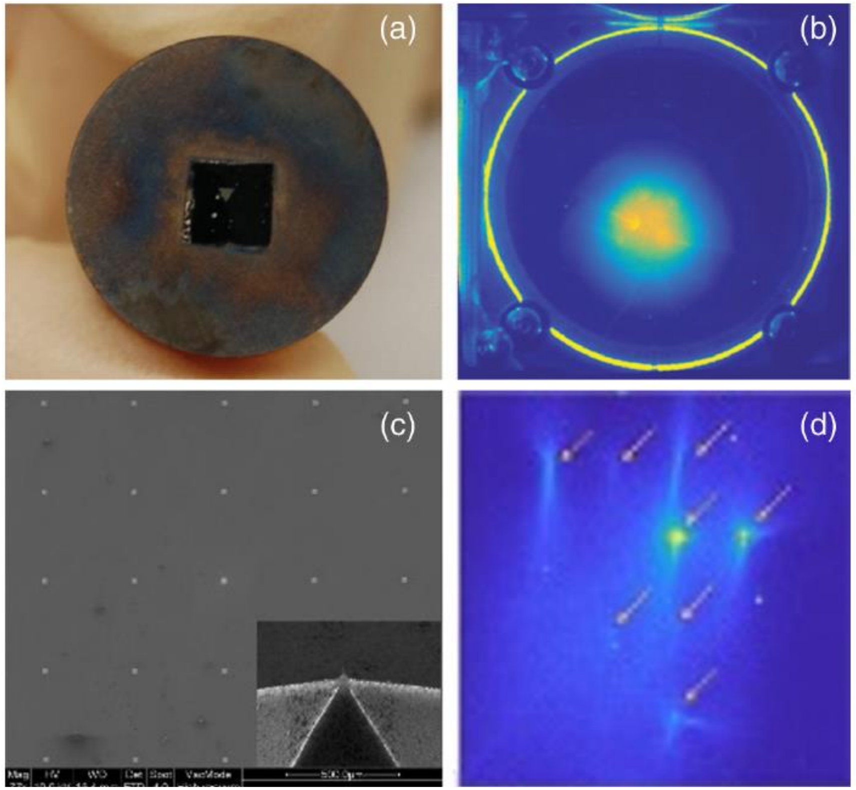

(a) Photograph of an FEA cathode with a triangular array inside a central square area of a round cathode plug and (b) beam image. (c) SEM image of a diamond tips (inset), and (d) beam image.
From Andrews et al., 2020, and Nichols et al., 2020.

Thermionic Emission Cathodes

- The TE cathode gun is one of the simplest and most robust electron sources; it is the workhorse of light source facilities around the world.
- TE cathode gun has not been used for the more demanding application of driving FELs, due to its lower transverse beam brightness and difficulty in achieving a short pulse.
- However, researchers at SACLA (Asaka et al., 2017) developed a low-emittance
- thermionic-gun-based injector. In the injector, electron beams are emitted from a CeB6 thermionic cathode of 3 mm diameter located in a dc 500-kV gun followed by a beam chopper and a bunch compressed to produce an electron beam with a high peak current (3 to 4 kA) and a low transverse normalized-slice emittance (below 1 μm) sufficient to drive a compact free electron laser.

Photocathode Electron Beam Shaping

- The distribution of an electron bunch emitted by a photocathode can be controlled via drive-laser shaping.
- Smooth transverse distribution:
  - Microlens-arrays (MLA)
  - Deformable mirrors:
    - an array of electrically adjustable small mirrors
  - Spatial light modulators
- Transversely shaped distribution:
  - Optical masks;
  - MLA;
- Longitudinally shaped distribution:
  - Frequency-domain: Dazzler in IR, etc
  - Time-domain: pulse stacker;
- Spatiotemporal 3D shaping: to be demonstrated in UV

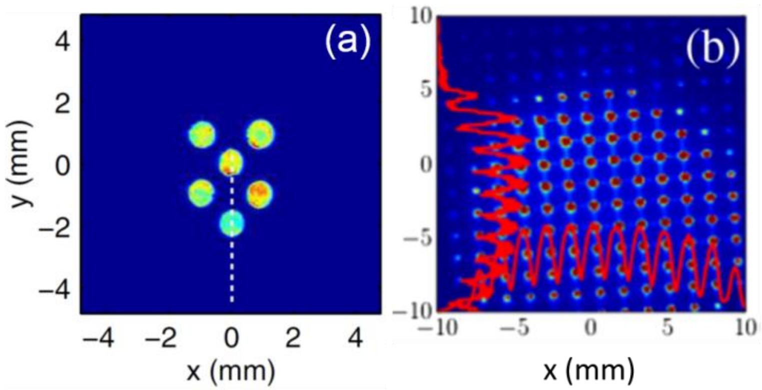

Transversely shaped electron-bunch distributions from
a photocathode. (a) an optical mask and (b) a MLA. From Rihaoui et al., 2009,Wisniewski et al., 2012.

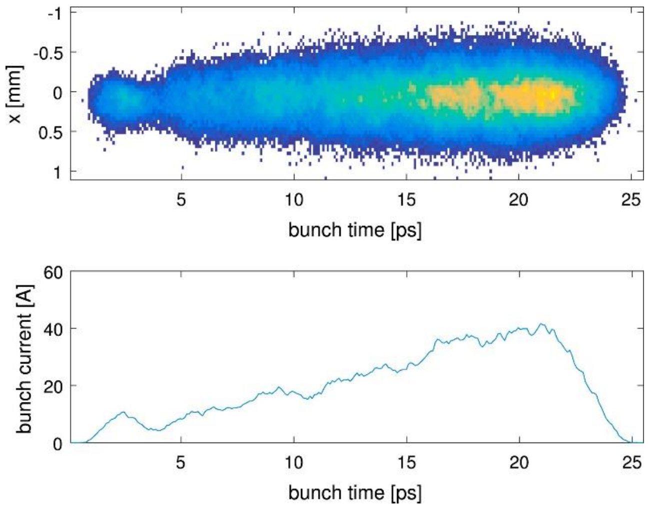

Measured double-triangular electron bunch generated with α-BBO laser pulse stacking. Top panel: x-z projection of the
bunch on a screen. Bottom panel: corresponding current profile. From Loisch et al., 2018.

Beam Control in 1-D Using External Fields

Generation of shaped current: local coupling combined with transverse masking.

- Dogleg beamline with a mask:

  Example: At ATF, an incoming bunch with a longitudinal phase-space chirp was sent to a dispersive section. A transverse mask (eg, tungsten wire) is inserted in the dispersive section (dispersion=1.5 m) to modify the final beam longitudinal shape.

  Fig on the right: Experimental generation of a sub-picosecond bunch train at the ATF using a dogleg beamline with final beam distribution in a downstream spectrometer and a measured temporal distribution via interferometry of coherent transition radiation. (Muggli et al., 2008, and Muggli, Allen,Yakimenko, Park et al., 2010.)

- The dipole magnets used to create the dispersive section can be replaced by a couple of transverse mode cavity, which can also create a spatiotemporal coupling.

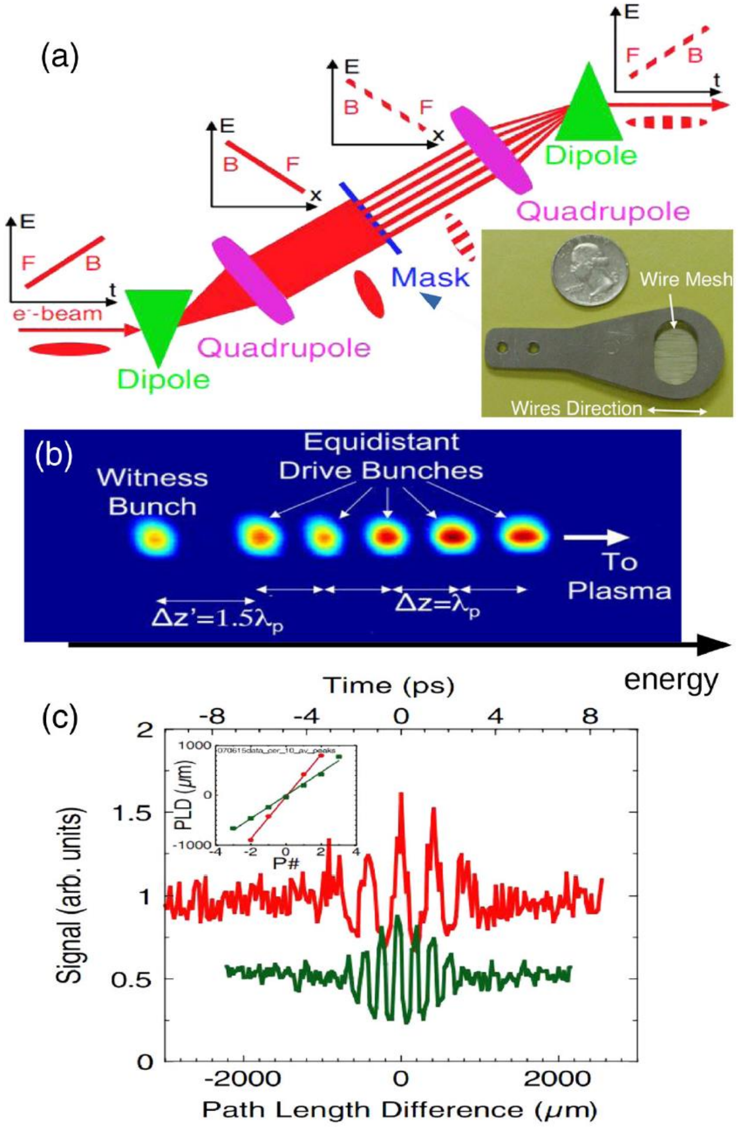

Current-shaping using transverse deflecting cavities

- Transverse cavities can directly introduce a spatiotemporal coupling (Zholents et al., 1999; Kur et al., 2009).
- The shaping method does not suffer from CSR-induced phase-space degradation. It can also provide control over the LPS chirp.

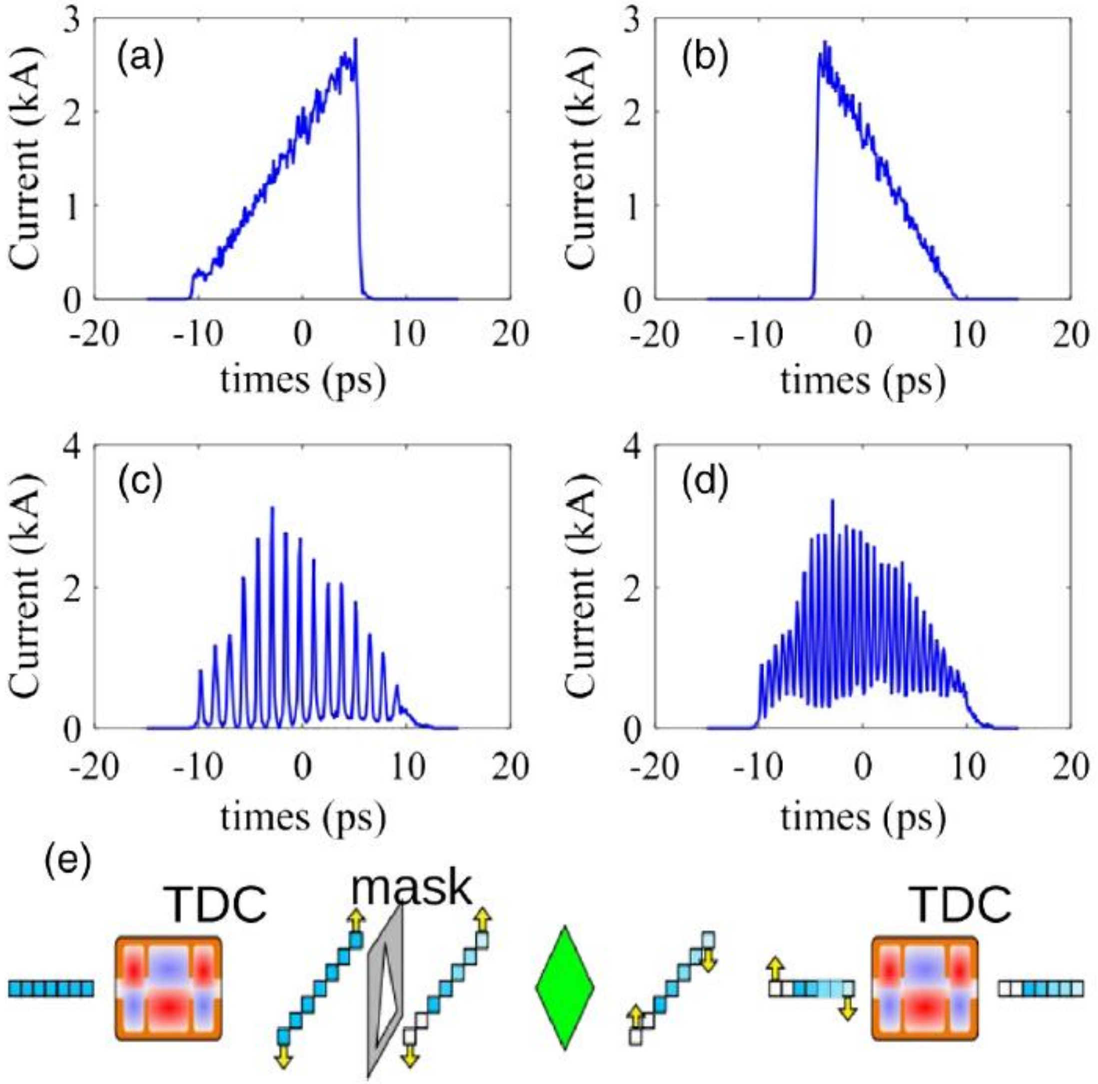

Example: The generation of (a) ramped, (b) reverse-triangle, and (c), (d) modulated bunch distributions using local correlations (e) imparted by a pair of transverse deflecting cavities (TDCs) combined with different masks. The shaping mask is located between the two TDCs and with sufficient phase advance from the upstream TDC to ensure that the beam has a significant xz correlation at its location. Adapted from Ha et al., 2020.

Bunch longitudinal compression using a dogleg/chicane

To compress a bunch longitudinally, a dogleg/chicane can be used. A linear longitudinal phase space correlation is needed.

There is a non-linear correlation part from higher orders of the rf field:

(1) Can be dealt with non-linear dispersion (by adding sextupoles for example) in the dogleg; or

(2) Can be controlled by using multi-frequency rf acceleration prior to the dogleg.

(3) Can be pre-compensated via photocathode drive-laser temporal shaping.

(4) The above methods can be mixed and combined to achieve the final longitudinal beam distribution.

Examples are given in the next slide.

Phase-space shaping via introduction of nonlinear longitudinal dispersion at the NEPTUNE and (b),(d) the resulting LPS with (c),(e) the current distribution. England, Rosenzweig, and Travish, 2008.

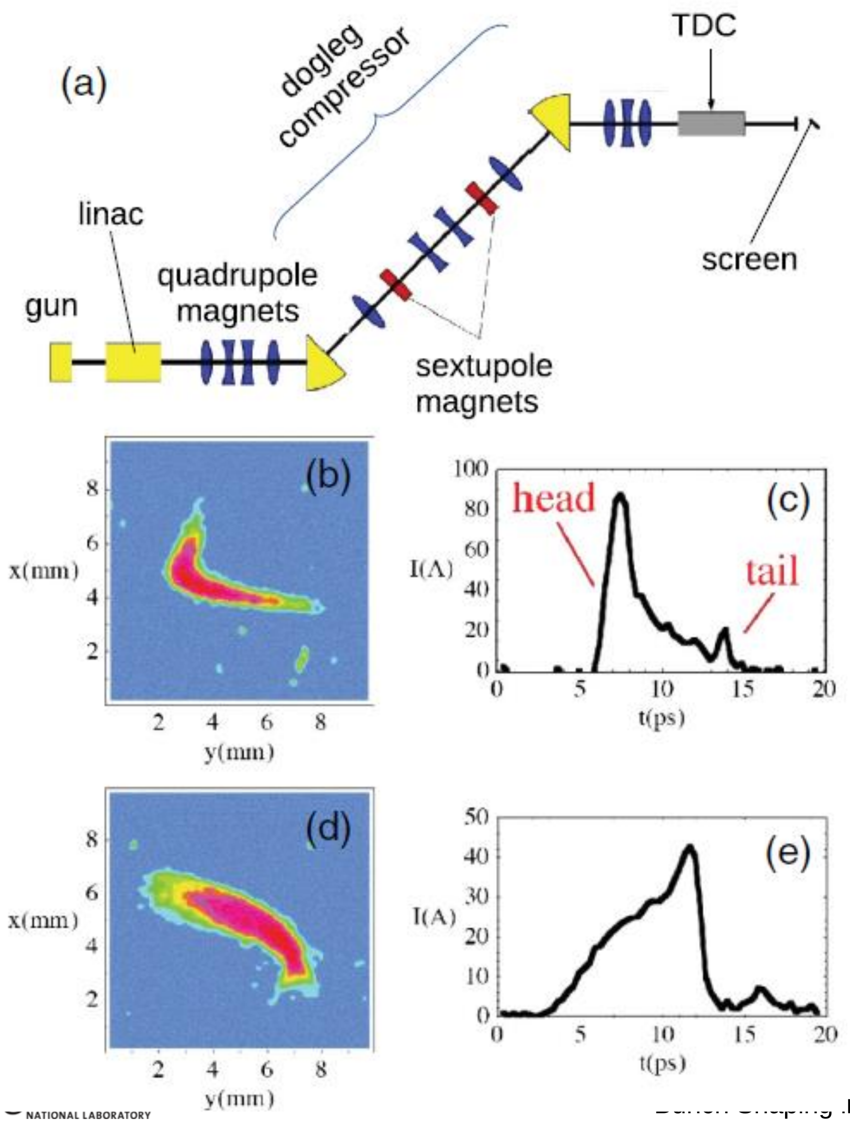

Example: a dual-frequency linac at the FLASH, DESY with (b) nominally compressed beam and (c) linearly ramped bunch via dual frequency linac. (Piot et al., 2012.)

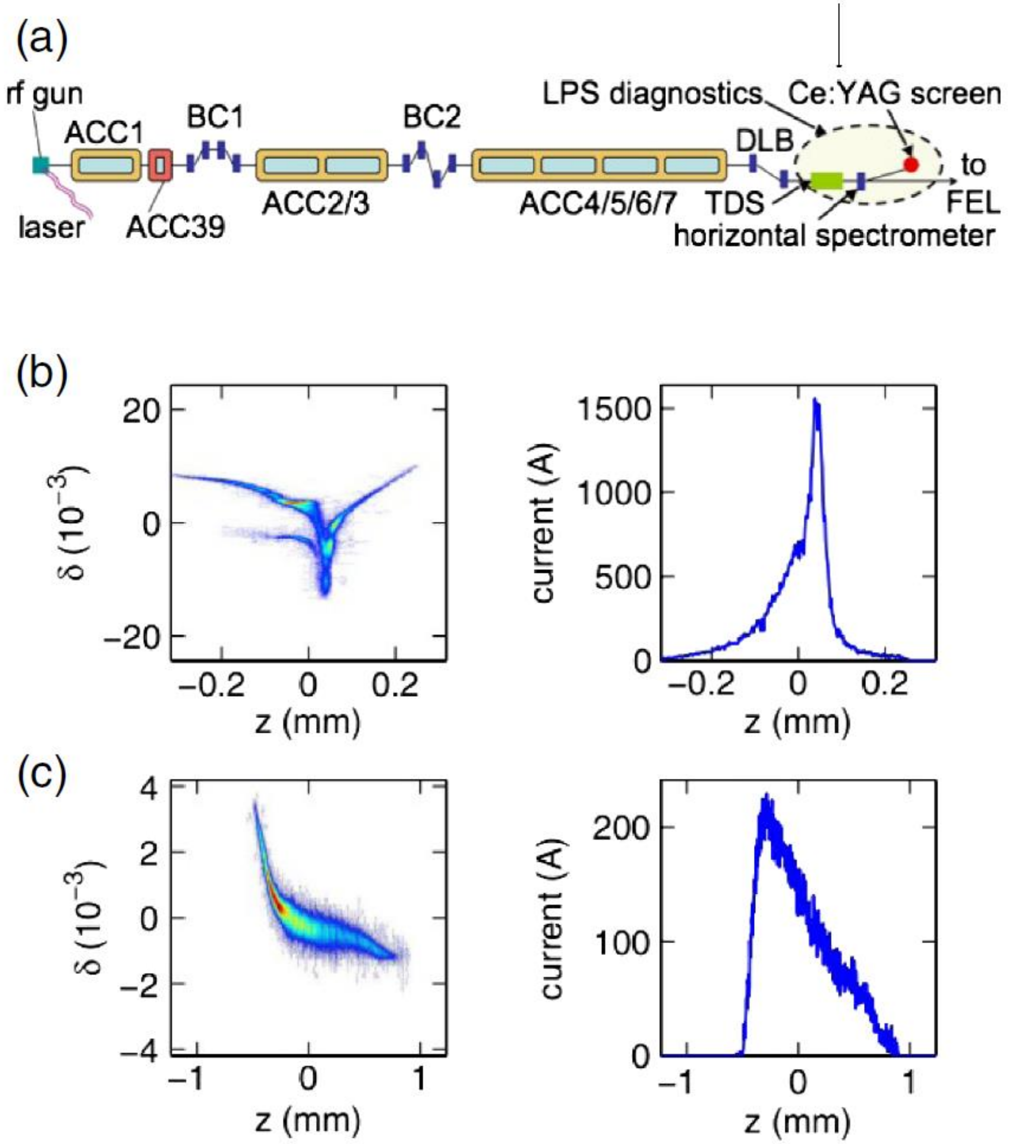

Controlling longitudinal phase space (LPS) correlation

- Longitudinal chirp control is conventionally achieved by accelerating beam off the rf crest.
- A LPS chirp control method using several deflecting cavities was introduced by Yampolsky, Simakov, and Malyzhenkov (2020)
- Efficient → the introduced chirp scales quadratically with the cavity's strength κ, while the off-crest acceleration scales linearly with the accelerating field.

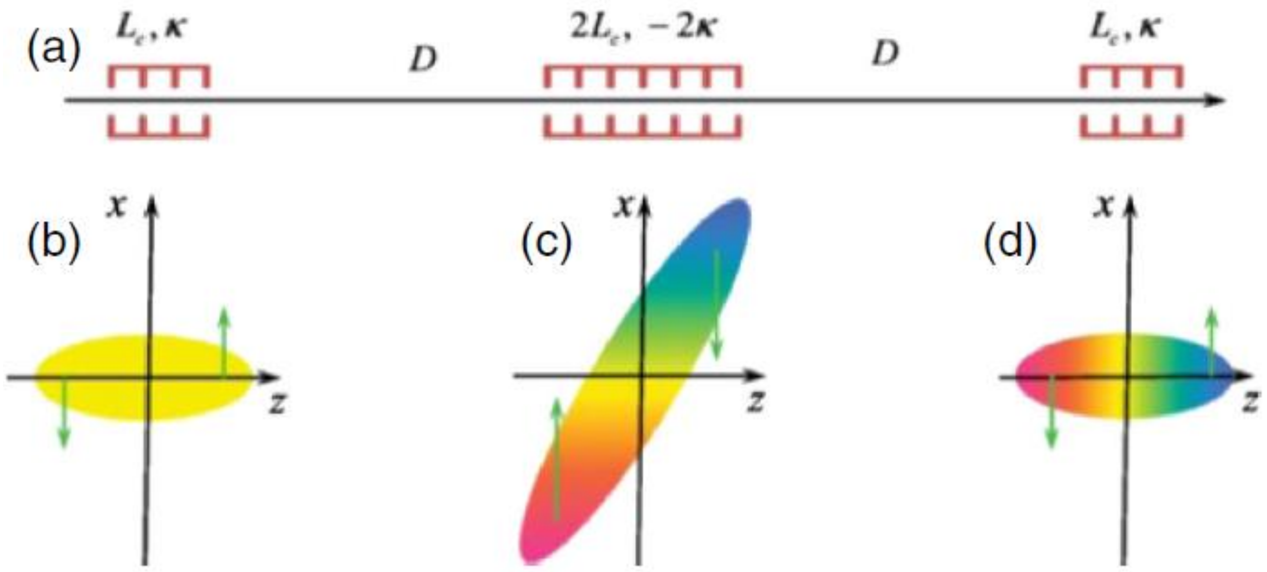

(a) ATDC-based beamline for the generation of strong LPS chirps. (b)–(d) The x − y electron-bunch distribution inside each TDC with the arrows gives the direction of the transverse kick x0. The color map indicates the energy distribution.

Yampolsky, Simakov, and Malyzhenkov, 2020.

Controlling longitudinal phase space (LPS) correlation

- Higher harmonic rf can be used to control the nonlinear chirp. For example, correcting or imposing quadratic nonlinearities in the LPS can be achieved by combining a harmonic rf field to the fundamental mode.

Example of longitudinal phase-space linearization at the LCLS facility. The LPS measurement (a) without and (b) with operation of the fourth-harmonic linearizing cavity (operating at 11.424 GHz).

Akre et al., 2008.

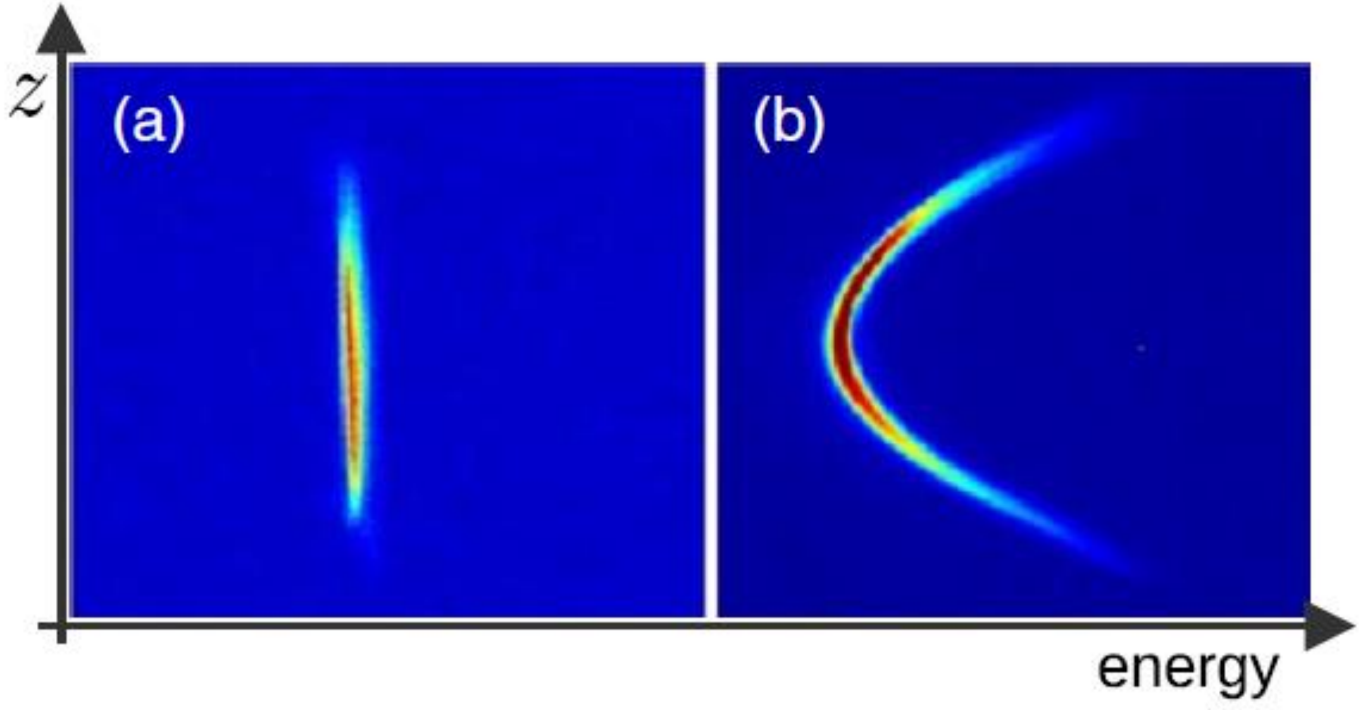

Longitudinal shaping with beam self-generated field

- Single-bunch: operating with laser and gun parameters in a “blowout regime” (where all particles experience a similar space-charge field strength) to evolve into an ellipsoidal beam: “pancake”, “cigar”.
- Multi-bunch:
  - By shaping the drive-laser into three longitudinally spaced pulses, a main bunch is sandwiched by two “field-shaping” bunches which generates a nearly linear longitudinal chirp in the main bunch (head particles has lower energy). The main bunch consequently goes through a drift and is compressed ballistically.
  - Multi-bunches generated by multi-pulses of drive laser go through plasma oscillation, bunch train intensity modulation at a certain location is determined by plasma phase advance.
- Bunch shaping using wake field

  Wakefield can be used to control the longitudinal phase-space correlation. This can be used for bunch compression, shaping, or for energy de-chirp, or as a linearizer for longitudinal phase-space.

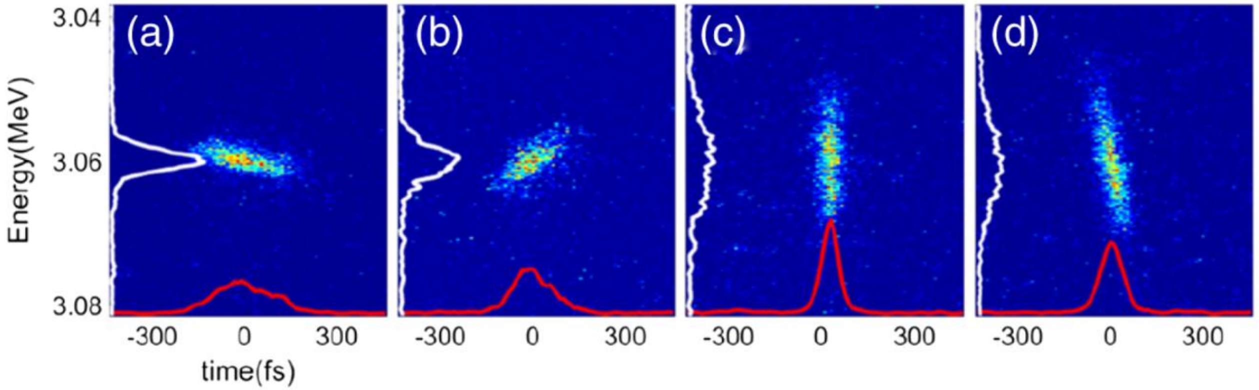

Example: Wakefield-based bunch compression using terahertz structure with a drive bunch. A measured longitudinal phase space of the target bunch and corresponding projections for different drive bunch charges. Zhao et al., 2018a.

Coupling between phase-spaces for bunch control

- Next we will discuss shaping methods that rely on the coupling between phase spaces associated with different degree of freedoms.
- Beamlines that have strong coupling or can swap phase-space coordinates.
- This class of phase-space manipulation enables precise shaping of the beam phase space and opens a path to emittance repartition among the different phase-spaces.

Phase-Space and Emittance

- The common coordinate system used in particle accelerator physics is the Cartesian system (x,y,z):
  - Longitudinal coordinate z →along particle propagation direction;
  - Transverse coordinates x and y →Horizontal x and vertical y.
- Particle position (x,y,z) combined with its momentum (p_x,p_y,p_z) form its coordinates in the 6D phase space (x,p_x,y,p_x,z,p_z) :
  - Each particle is represented by a point, and all particles in a bunch occupy a volume.
- A figure of merit of the beam's projection in (x,p_x) subspace is the ***normalized rms emittance*** defined as:

$$\varepsilon_x^n = \frac{1}{mc}\sqrt{<x^2><p_x^2> - <xp_x>^2}$$

- ***Liouville's theorem***: for non-interactive particles, the volume occupied by a certain number of particles in the 6D phase space is constant.

$$\varepsilon_x^n \varepsilon_y^n \varepsilon_z^n = \mathrm{Const}$$

Trace Space and un-normalized emittance

- More extensively used are the derivatives of (x,y) with respect to z:
  - $x' = P_x/P_z$, $y' = P_y/P_z$
  - 4D Coordinate vector $U = \begin{bmatrix} x \\ x' \\ y \\ y' \end{bmatrix}$
- Un-normalized emittance

$$\varepsilon_x = \sqrt{<x^2><x'^2> - <xx'>^2}$$

- For relativistic beams (relativistic factors β and γ) with low energy spread, we have

$$\varepsilon_x = \frac{\varepsilon_x^n}{\beta\gamma}$$

Transfer Matrix

- The transverse motion of a particle in an accelerator without dissipative force can be written as the *Hill's equation*:

$$u'' + K(z)u = 0 \text{ where } u \text{ can be } x \text{ or } y.$$

- Suppose A(z) and B(z) are two independent solutions which satisfy the following boundary conditions:

$$A(z_0) = B'(z_0) = 1$$

$$A'(z_0) = B(z_0) = 0$$

- Any solution to the equation can be written as

$$\begin{bmatrix} u(z) \\ u'(z) \end{bmatrix} = \boxed{\begin{bmatrix} A(z) & B(z) \\ A'(z) & B'(z) \end{bmatrix}} \begin{bmatrix} u(z_0) \\ u'(z_0) \end{bmatrix} \equiv \boxed{M(z|z_0)} \begin{bmatrix} u(z_0) \\ u'(z_0) \end{bmatrix}$$

Transfer matrix from z_0 to z

Transfer Matrix: Properties and Examples

- The 2D transfer matrix can be extended to 6D.
- The determinant of the transfer matrix is unity.
- The transfer matrix satisfies the ***symplectic*** condition. In 6D:

$$\widetilde{M_6} J_6 M_6 = J_6 \text{, where } J_6 = \begin{bmatrix} J & 0 & 0 \\ 0 & J & 0 \\ 0 & 0 & J \end{bmatrix} \text{ and } J = \begin{bmatrix} 0 & 1 \\ -1 & 0 \end{bmatrix} \text{ is the 2x2 unit symplectic matrix.}$$

- For a constant $K(z) = k$

$$u'' + ku = 0$$

  - If $k > 0$

$$M(z|z_0) = \begin{bmatrix} \cos\varphi & \frac{\sin\varphi}{\sqrt{k}} \\ -\sqrt{k}\sin\varphi & \cos\varphi \end{bmatrix} \quad \text{Focusing quad: } \varphi = (z_1 - z_0)\sqrt{k}$$

  - If $k < 0$

$$M(z|z_0) = \begin{bmatrix} \cosh\varphi & \frac{\sinh\varphi}{\sqrt{|k|}} \\ \sqrt{|k|}\sinh\varphi & \cosh\varphi \end{bmatrix} \quad \text{Defocusing quad: } \varphi = (z_1 - z_0)\sqrt{|k|}$$

  - If $k = 0$

$$M(z|z_0) = \begin{bmatrix} 1 & z_1 - z_0 \\ 0 & 1 \end{bmatrix} \quad \text{Drift space}$$

Beam Matrix

- Consider a bunch of particles centered at the origin of the phase space, i.e., $\langle x_i \rangle$=0 etc. where ⟨ ⟩ represents taking the average;
- Beam matrix: the covariance matrix of the phase space coordinates U; for (x, x', y, y') subspace:

$$\Sigma = \langle U\tilde{U} \rangle = \begin{bmatrix} \langle x^2 \rangle & \langle xx' \rangle & \langle xy \rangle & \langle xy' \rangle \\ \langle x'x \rangle & \langle x'^2 \rangle & \langle x'y \rangle & \langle x'y' \rangle \\ \langle yx \rangle & \langle yx' \rangle & \langle y^2 \rangle & \langle yy' \rangle \\ \langle y'x \rangle & \langle y'x' \rangle & \langle y'y \rangle & \langle y'^2 \rangle \end{bmatrix}$$

  Emittance is the determinant of the beam matrix.

- The beam matrix propagates via

$$\Sigma(z) = M\Sigma(z_0)\tilde{M}$$

where M is the transfer matrix from z_0 to z.

Phase-Space Manipulation

Phase-Space Manipulation

- An electron beam directly out of a photoinjector does not always have the phase-space properties required in its applications.

- Phase-space manipulation is necessary to achieve certain beam distribution, for example:
  - the beam can be compressed longitudinally →higher peak current →FELs;
  - round beam → flat beam (to drive planar dielectric wakefield or planar radiation generation gratings etc…);
  - the longitudinal and transverse Emittances of the beam can be EXchanged (EEX);
  - when EEX is combined with the flat beam → repartition of emittances in 3D can be achieved;
  - the above manipulations are in the root-mean-square sense; the beam profiles can be more precisely tailored, such as bunch train or linearly ramped current etc. for higher transformer ratio in a wakefield accelerator etc.

- Aside from beam applications, other possible applications include beam diagnostics, bunch compression etc.

Round-to-Flat Beam Transformation

Round-to-flat beam transformation: Beam Matrix Formulation

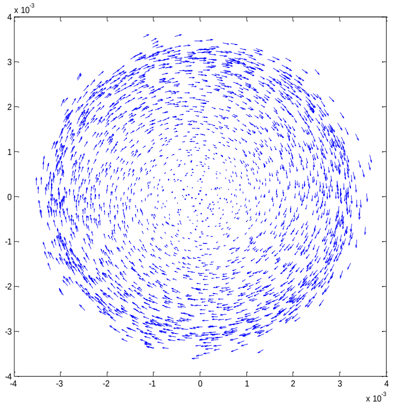

$$\Sigma_{round} = \begin{bmatrix} \varepsilon_{eff}\beta & 0 & 0 & L \\ 0 & \varepsilon_{eff}/\beta & -L & 0 \\ 0 & -L & \varepsilon_{eff}\beta & 0 \\ L & 0 & 0 & \varepsilon_{eff}/\beta \end{bmatrix}$$

General form of a round beam at beam waist location

$$\varepsilon_{eff} = \sqrt{\varepsilon_u^{\ 2} + L^2}$$

uncorrelated emittance

Const. related to canonical angular momentum $L=\frac{<L>}{2Pz}$

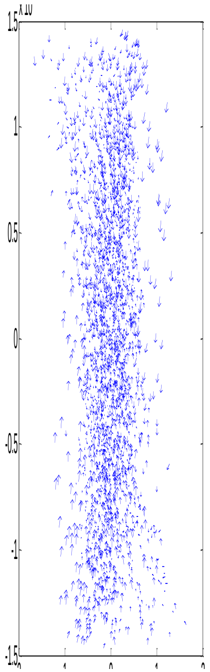

$$\Sigma_{flat} = M\,\Sigma_{round}\,\tilde{M}$$

Transfer matrix of the round-to-flat beam transformer

$$\Sigma_{flat} = \begin{bmatrix} \varepsilon_{-}\beta & 0 & 0 & 0 \\ 0 & \varepsilon_{-}/\beta & 0 & 0 \\ 0 & 0 & \varepsilon_{+}\beta & 0 \\ 0 & 0 & 0 & \varepsilon_{+}/\beta \end{bmatrix}$$

Flat beam emittances are given by:

$$\varepsilon_{\pm} = \sqrt{\varepsilon_u^{\ 2} + L^2} \pm L$$

e.g. L=20 mm mrad, ε_u=1 mm mrad
ε_+=47 mm mrad; ε_-=0.02 mm mrad

For $L \gg \varepsilon_u$, We have $\varepsilon_{-} = \frac{\varepsilon_u^{\ 2}}{2L} << \varepsilon_u$

Flat beam emit. could be smaller than thermal emit.

Round-to-flat transfer matrix building blocks: skew quads and drifts

Round beam: emittance ratio =1 but with large x-y coupling via angular momentum.
Flat beam: large transverse emittance ratio, zero average angular momentum.

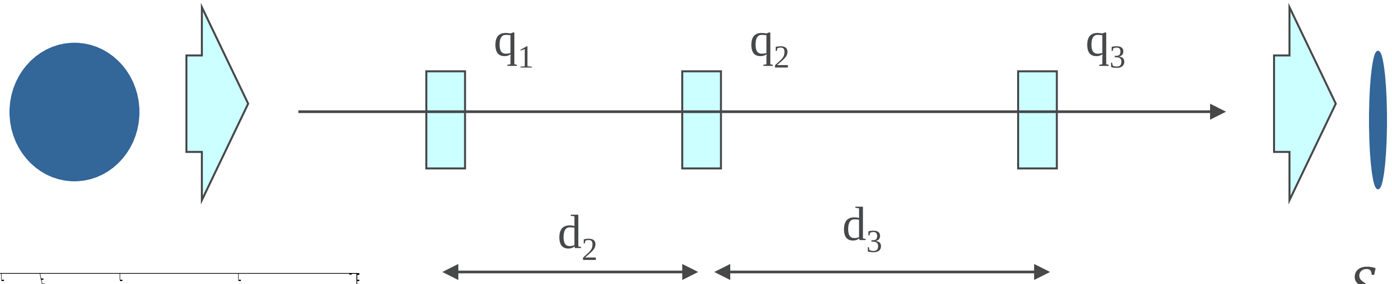

$$\langle \tau \rangle_{total} = 2 \cdot \sum q_i \langle x_i \; y_i \rangle$$

$$S = \frac{1}{\varepsilon} \begin{bmatrix} \langle xx' \rangle & -\langle x^2 \rangle \\ \langle x'^2 \rangle & -\langle xx' \rangle \end{bmatrix}$$

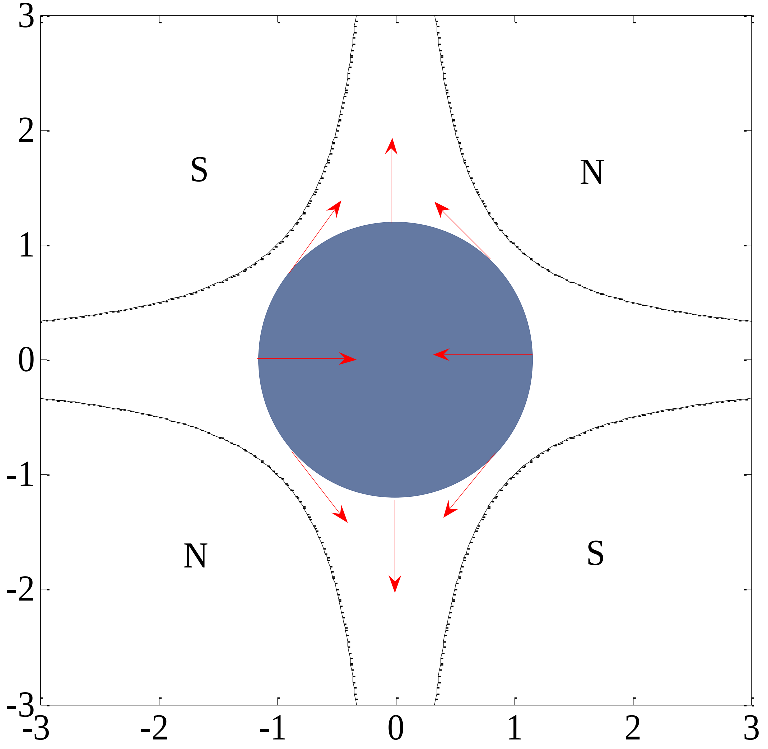

Two sets of solutions:

$$q_1 = \pm \sqrt{\frac{-d_2 S_{11} + S_{12} - d_2 d_T S_{21} + d_T S_{22}}{d_2 d_T S_{12}}}$$

$$q_2 = -\frac{S_{12} + d_T S_{22}}{d_2 d_3 (1 + S_{12} q_1)}$$

$$q_3 = -\frac{q_1 + q_2 + d_2 S_{11} q_1 q_2 + S_{21}}{1 + (d_T q_1 + d_3 q_2) S_{11} + d_2 d_3 q_2 (S_{21} + q_1)}$$

(D. Edwards)

Round-to-flat Beam transformation: the Round Beam
Three difference dynamic regimes

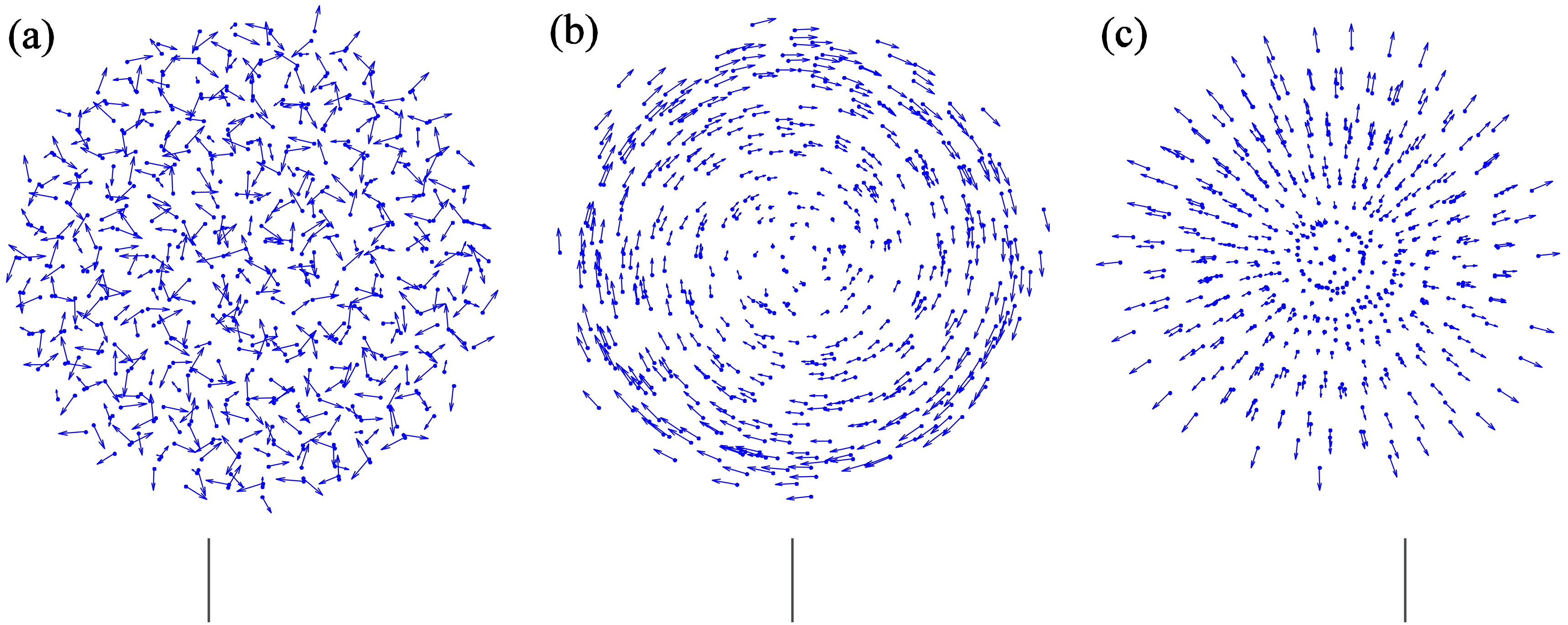

emittance | canonical angular momentum | space charge

envelope equation in a drift: $\sigma'' - \frac{\varepsilon^2}{\sigma^3} - \frac{L^2}{\sigma^3} - \frac{K}{4\sigma} = 0$ where $K = \frac{2I}{I_0 \beta^3 \gamma^3}$.

Round-to-Flat Beam Transformation

- Generation of an angular-momentum-dominated beam by immersing the cathode in a high longitudinal magnetic field;

Removal of the angular momentum via a set of quadurpoles to obtain a flat beam.

$$\varepsilon_n^{\pm} = \sqrt{\varepsilon_n^{\ 2} + L^2} \pm L$$

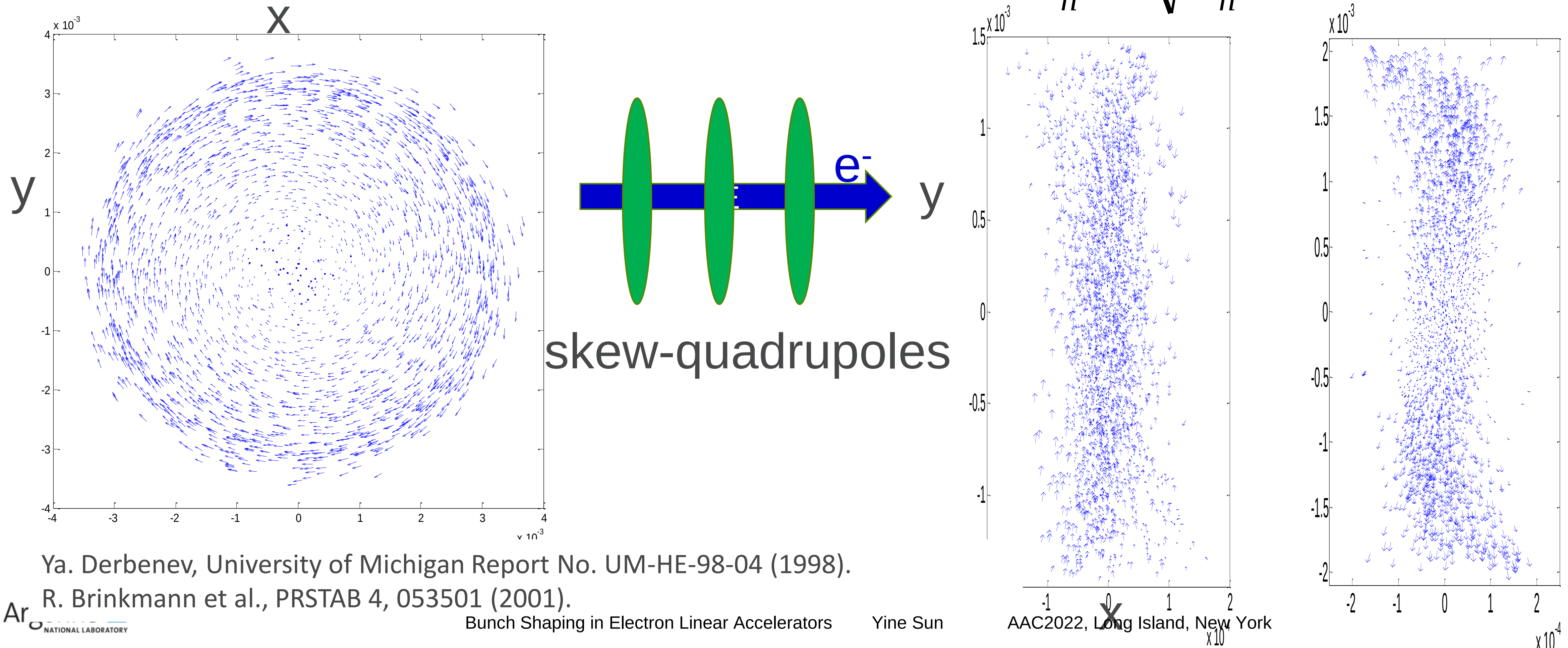

Ya. Derbenev, University of Michigan Report No. UM-HE-98-04 (1998).
R. Brinkmann et al., PRSTAB 4, 053501 (2001).

Round-to-Flat Beam Transformation Demonstration: Fermilab/NICADD Photoinjector Lab. (FNPL) (a.k.a. A0)

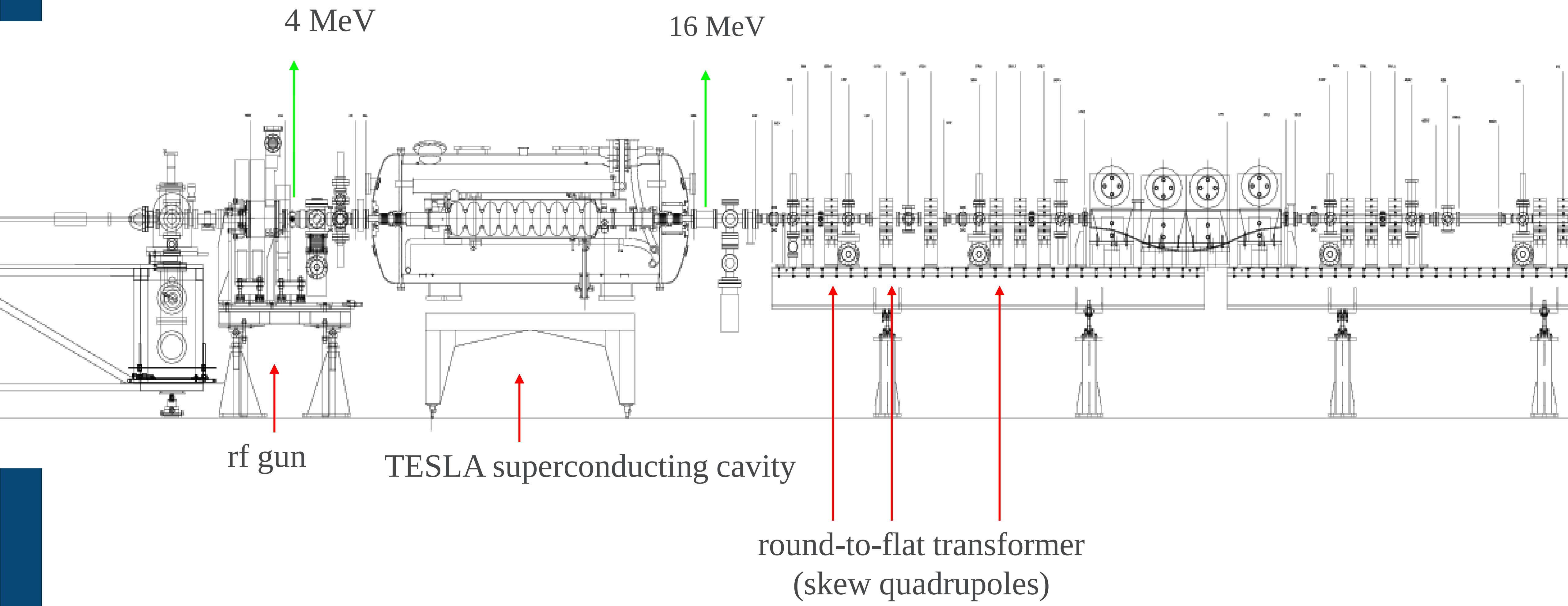

Generation of angular momentum dominated e$^-$ beam

$$L = \gamma m r^2 \dot{\phi} + \frac{1}{2} e B_z r^2$$

On the photocathode: $\langle L \rangle = e B_0 \sigma_c^2$

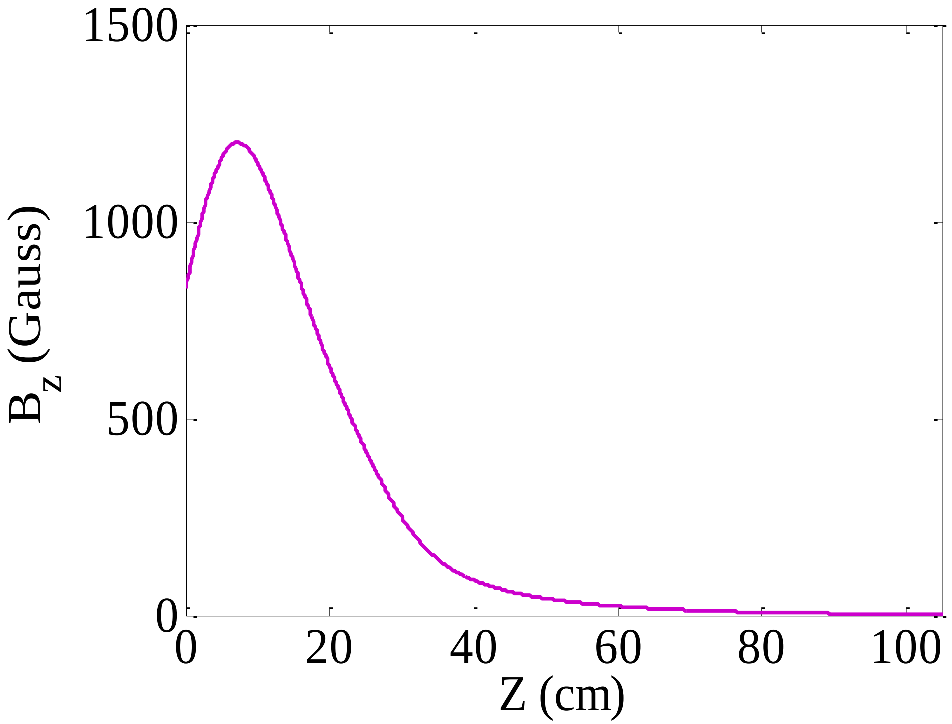

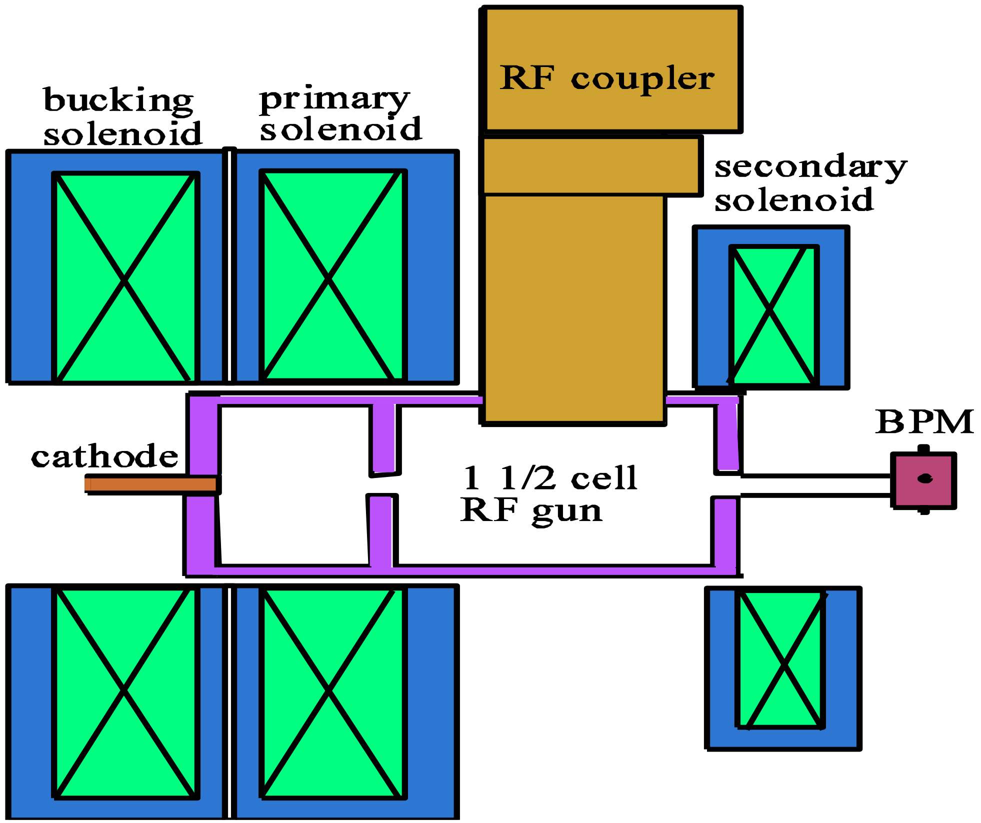

FNPL 1.625-cell RF gun, 1.3 GHz

Solenoidal end field applies a torque to the beam.

When B_z=0, canonical = mechanical angular momentum.

Measurement of canonical angular momentum on the cathode

$$\langle L \rangle = eB_0\sigma_c^2$$

B_0: B-field on cathode
σ_c :RMS beam size on cathode

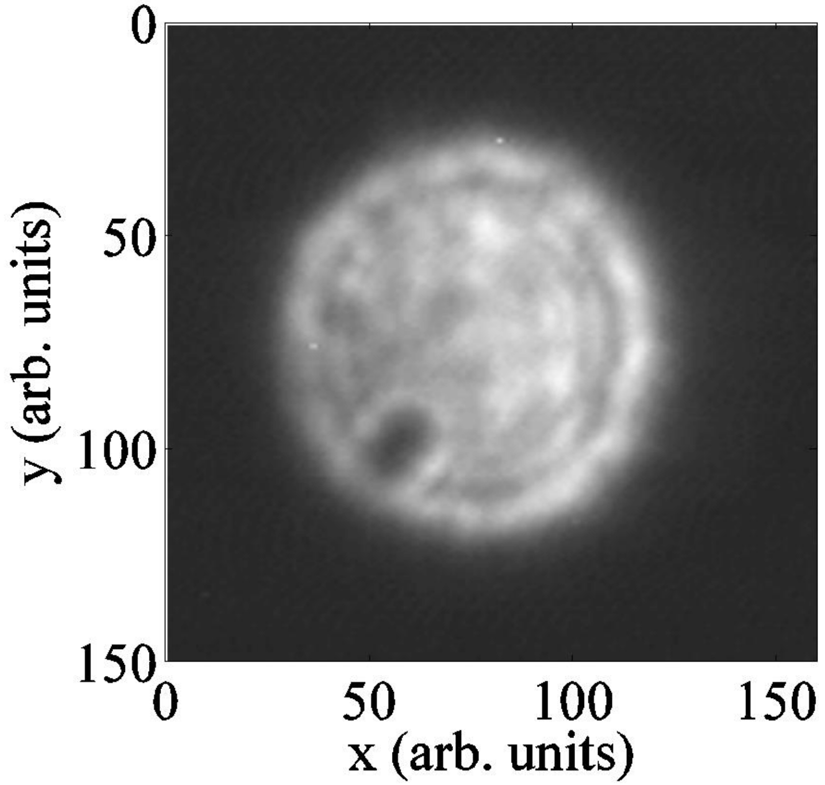

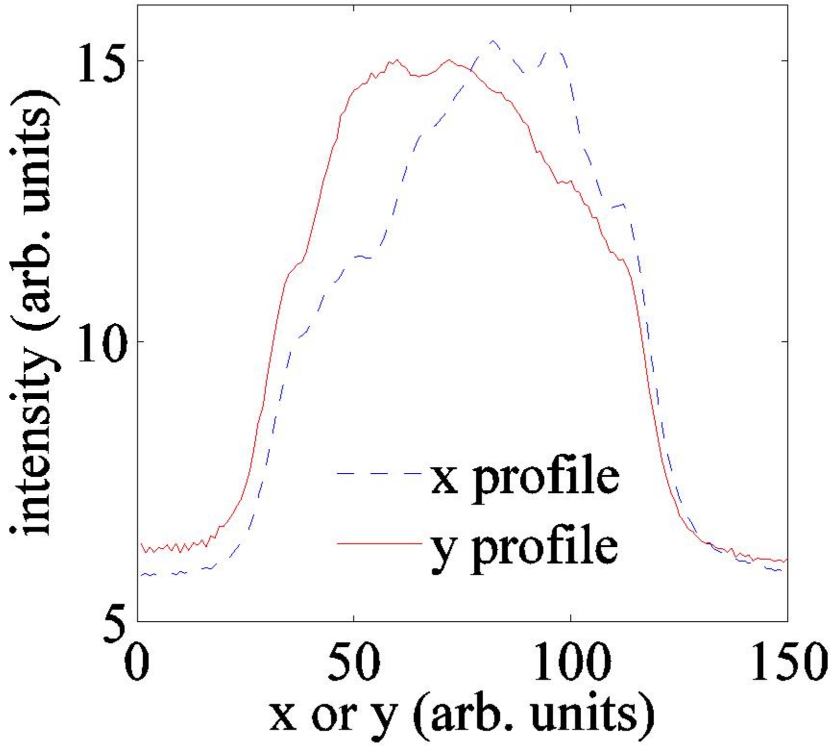

Measurement of canonical angular momentum in a drift

Insert flag or slits at Z1→
Measure beam size σ_1 at Z1
Insert flag at Z2→
Measure beam size σ_2 and slits rotation angle θ at Z2

$$\langle L \rangle = 2 p_z \frac{\sigma_1 \sigma_2 \sin\theta}{D}$$

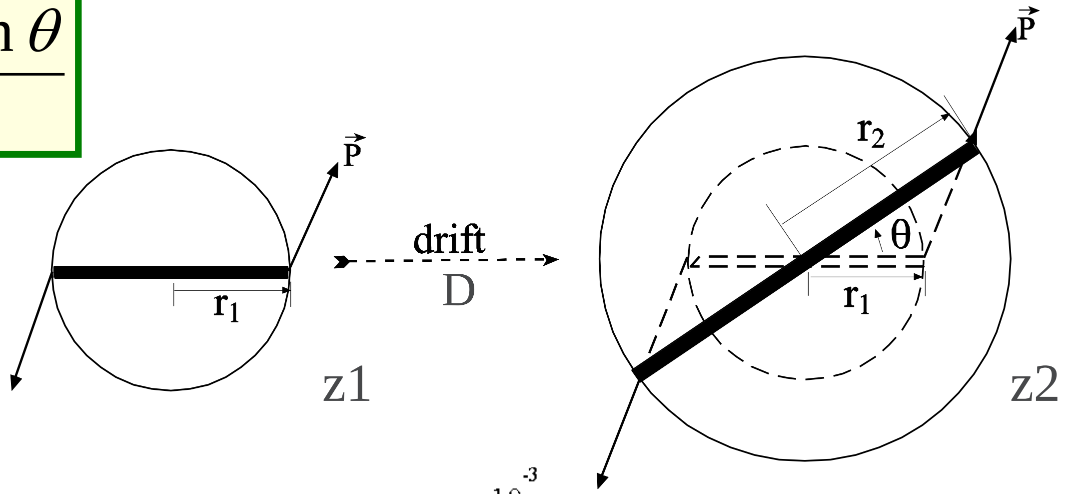

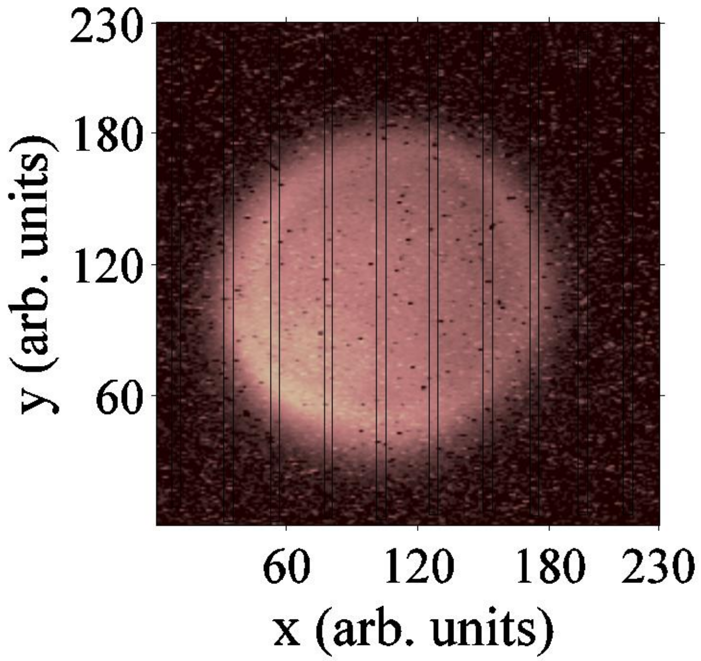

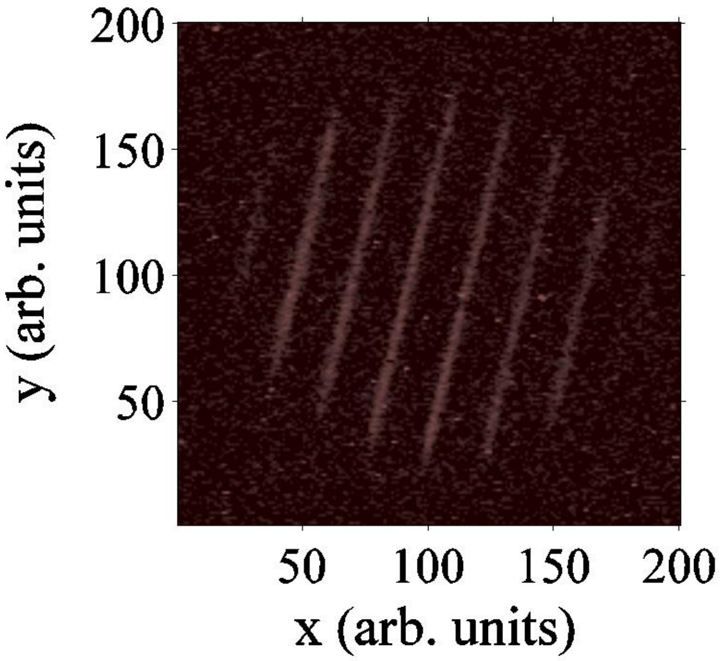

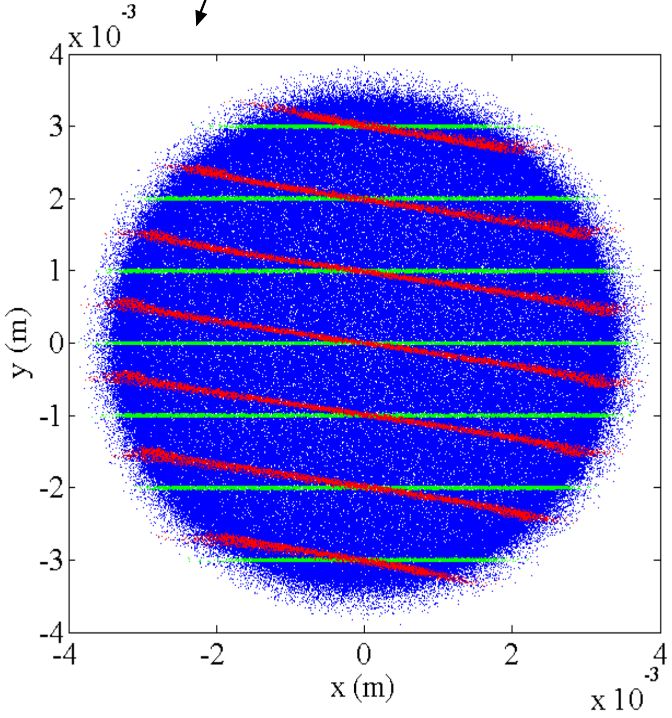

Demonstration of conservation of canonical angular momentum

as a function of magnetic field on cathode

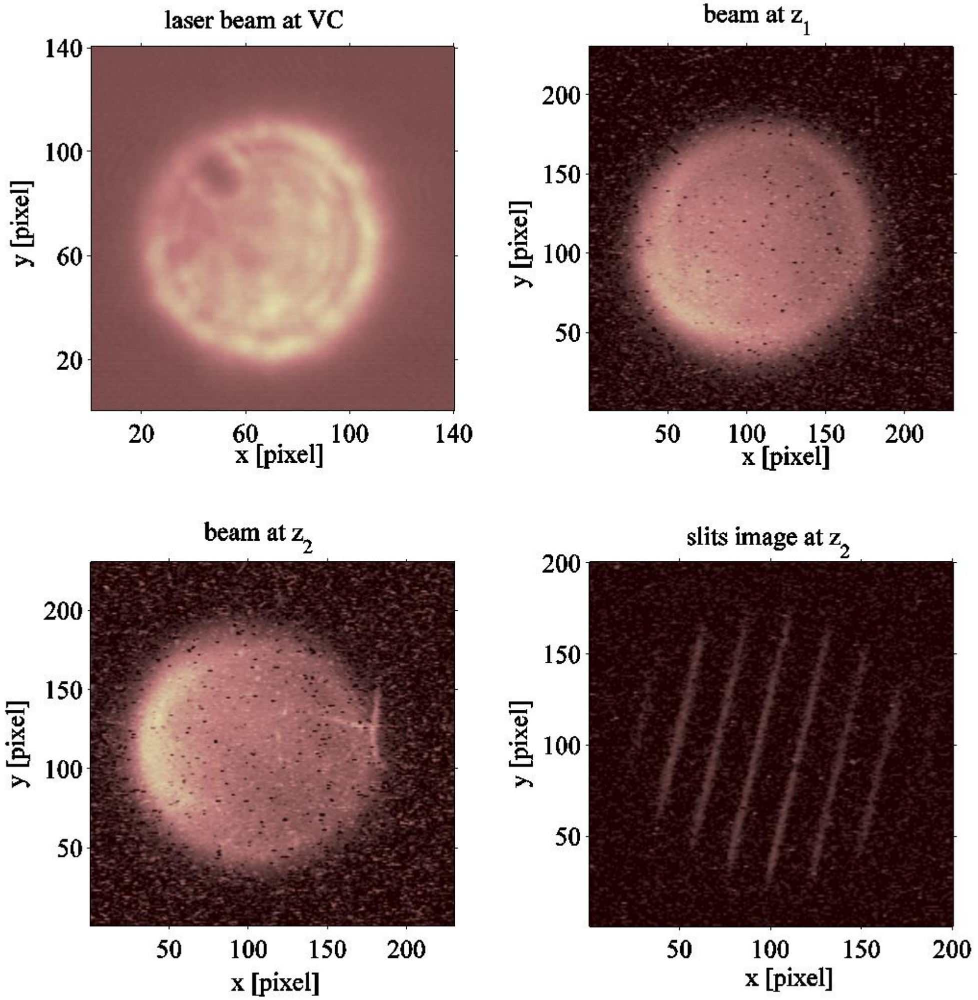

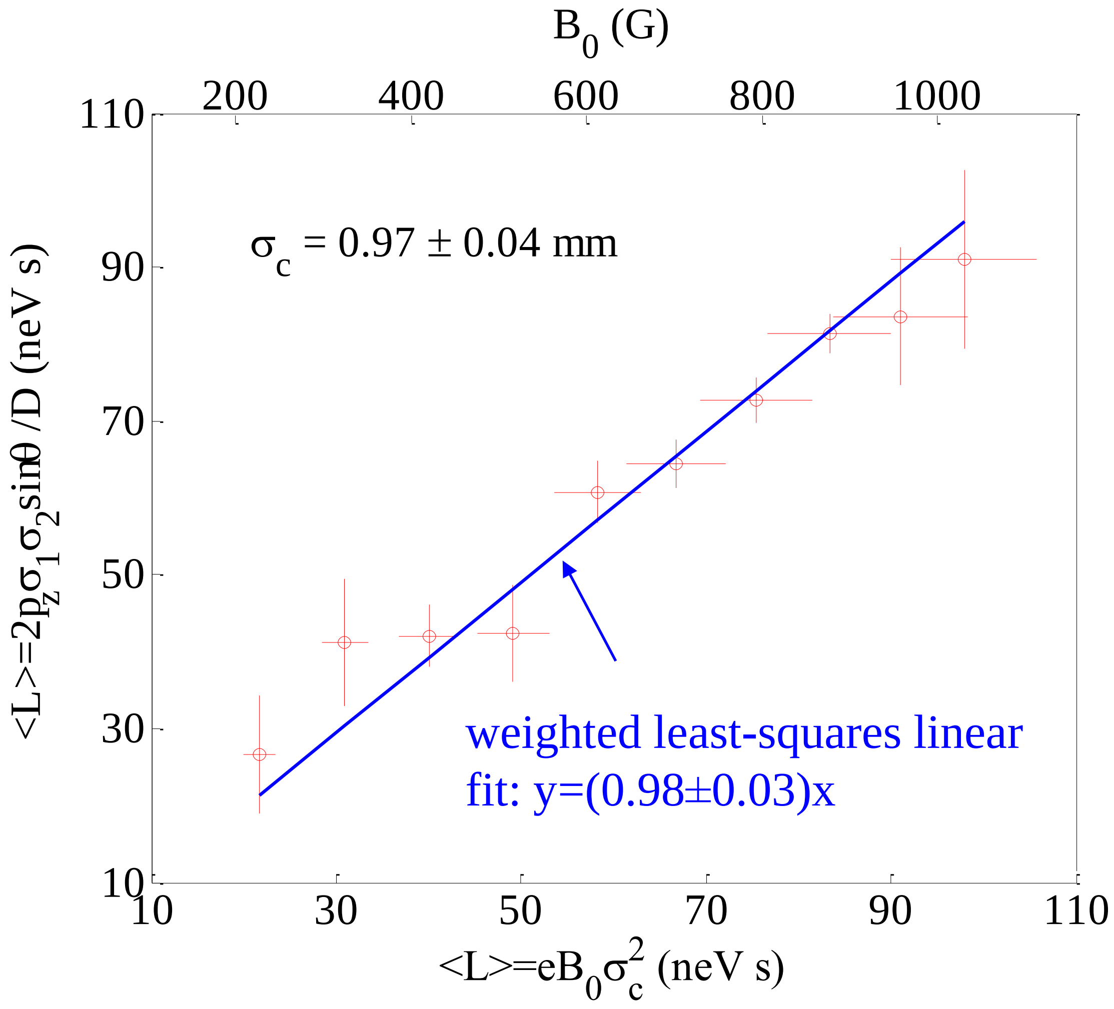

Parametric dependencies of the angular momentum

- Angular momentum versus
  - beam longitudinal position z
  - bunch charge
  - beam size on the cathode

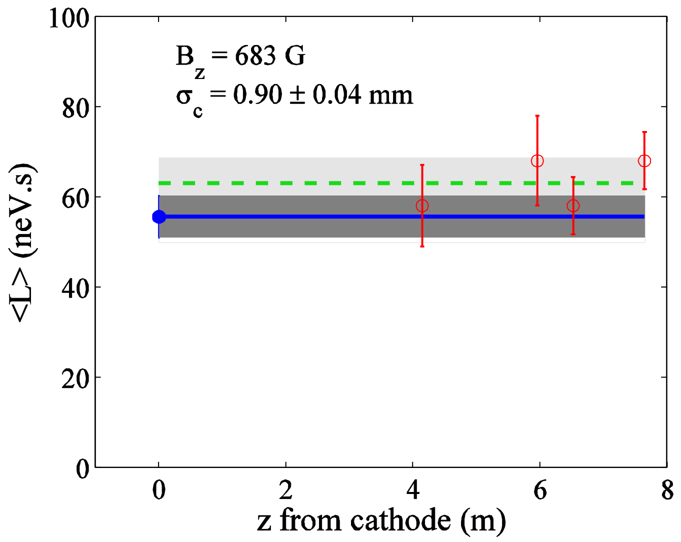

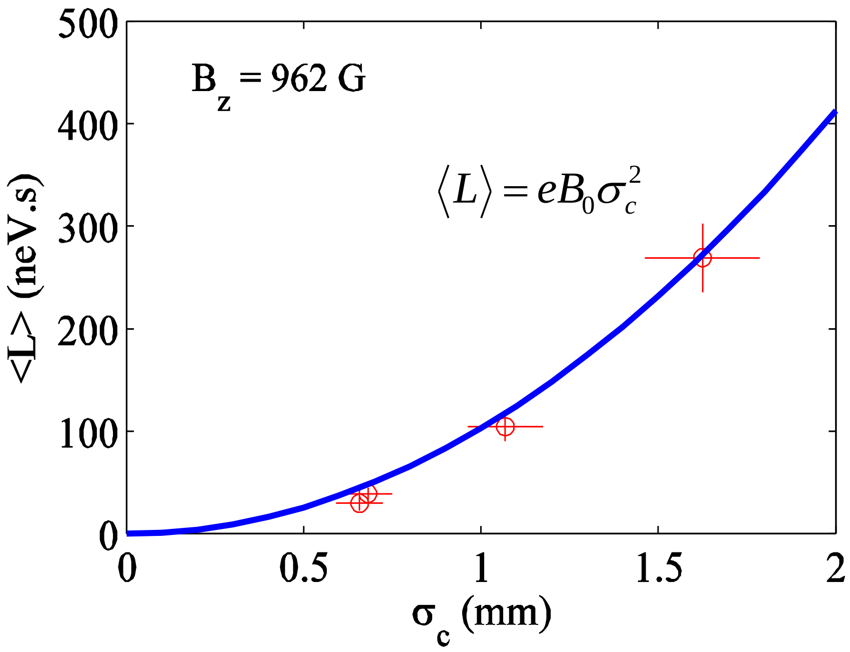

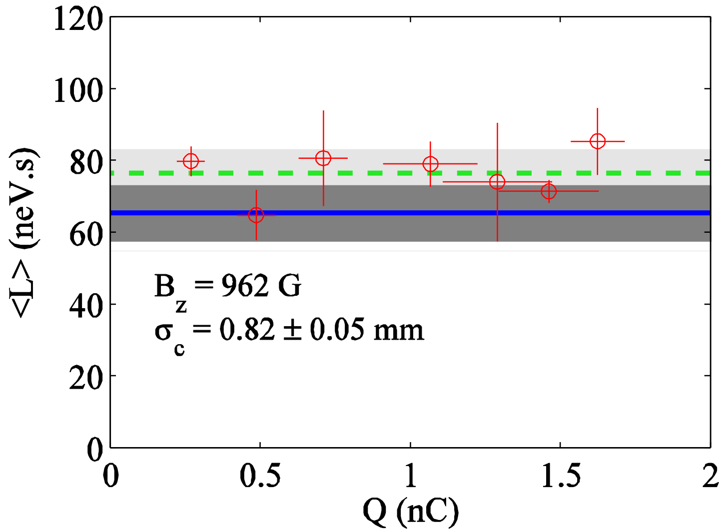

Position and velocity snap shots at the entrance/exit of the transformer

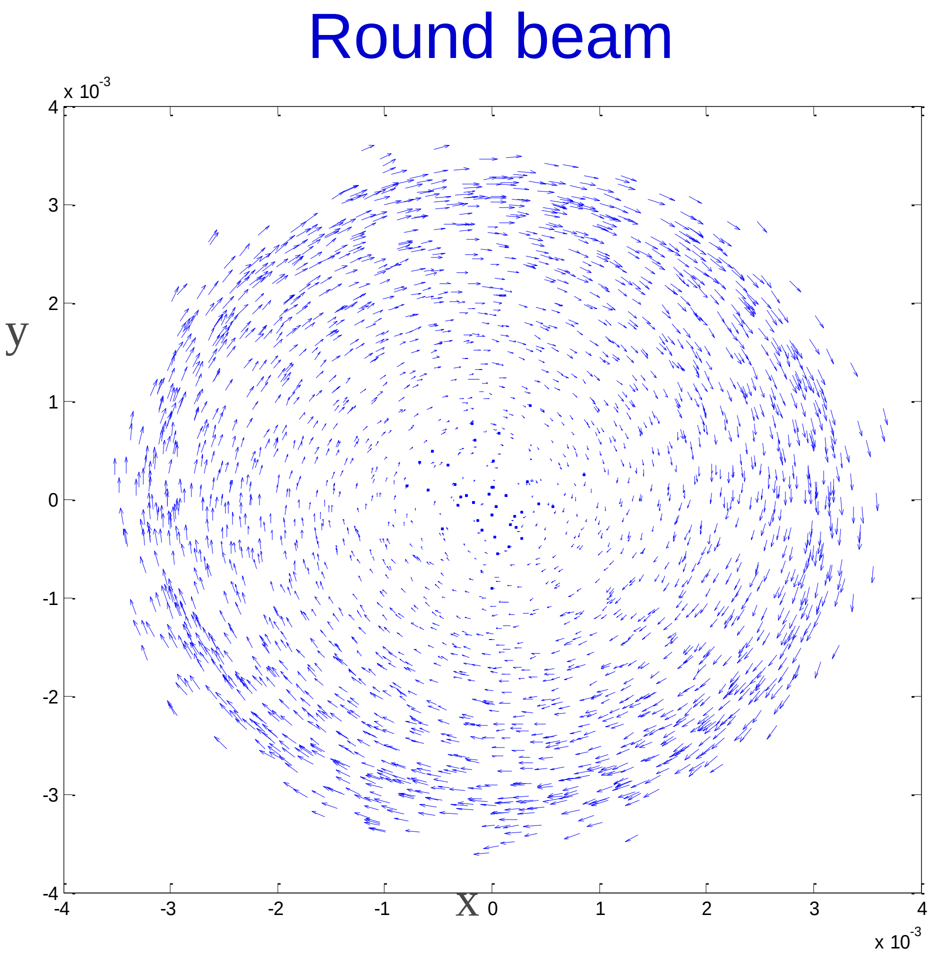

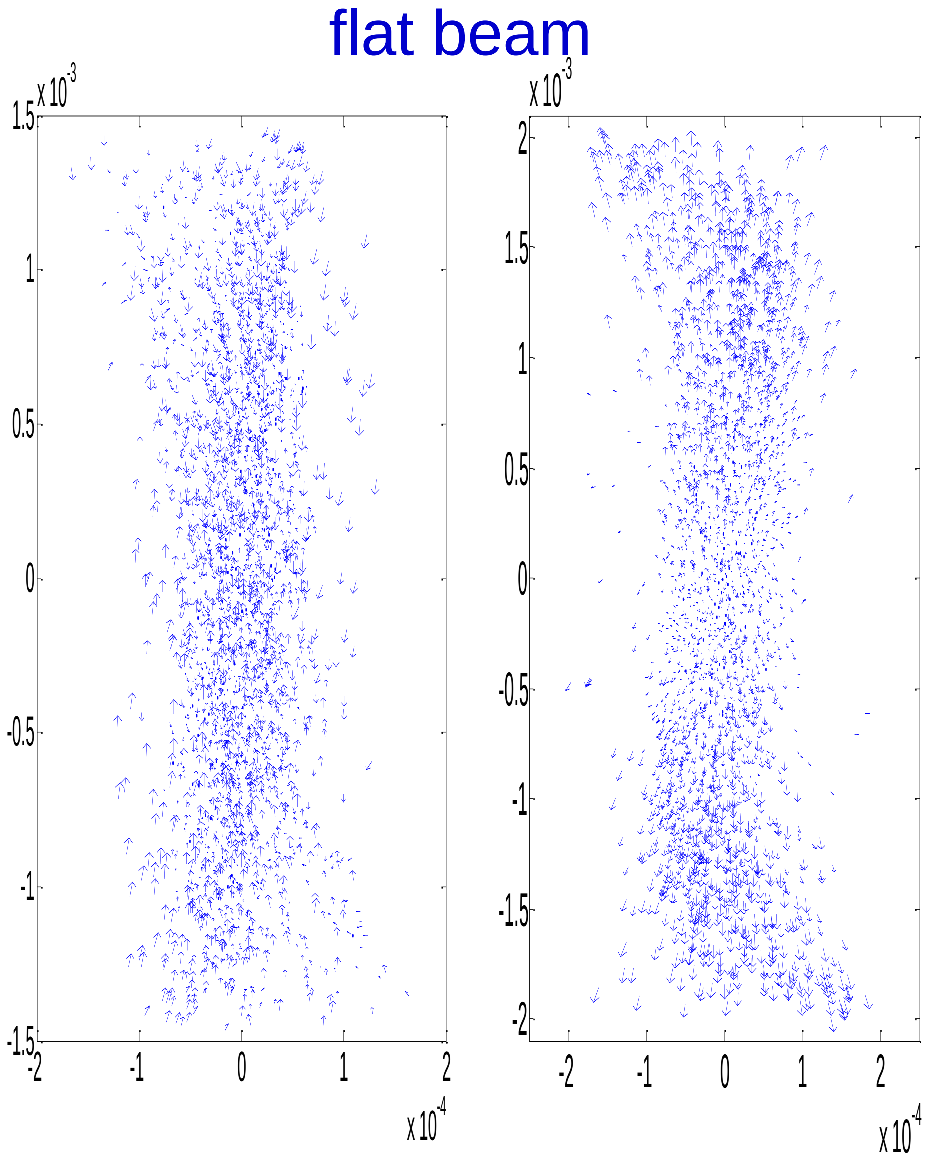

Beam evolution through the transformer for the first solution

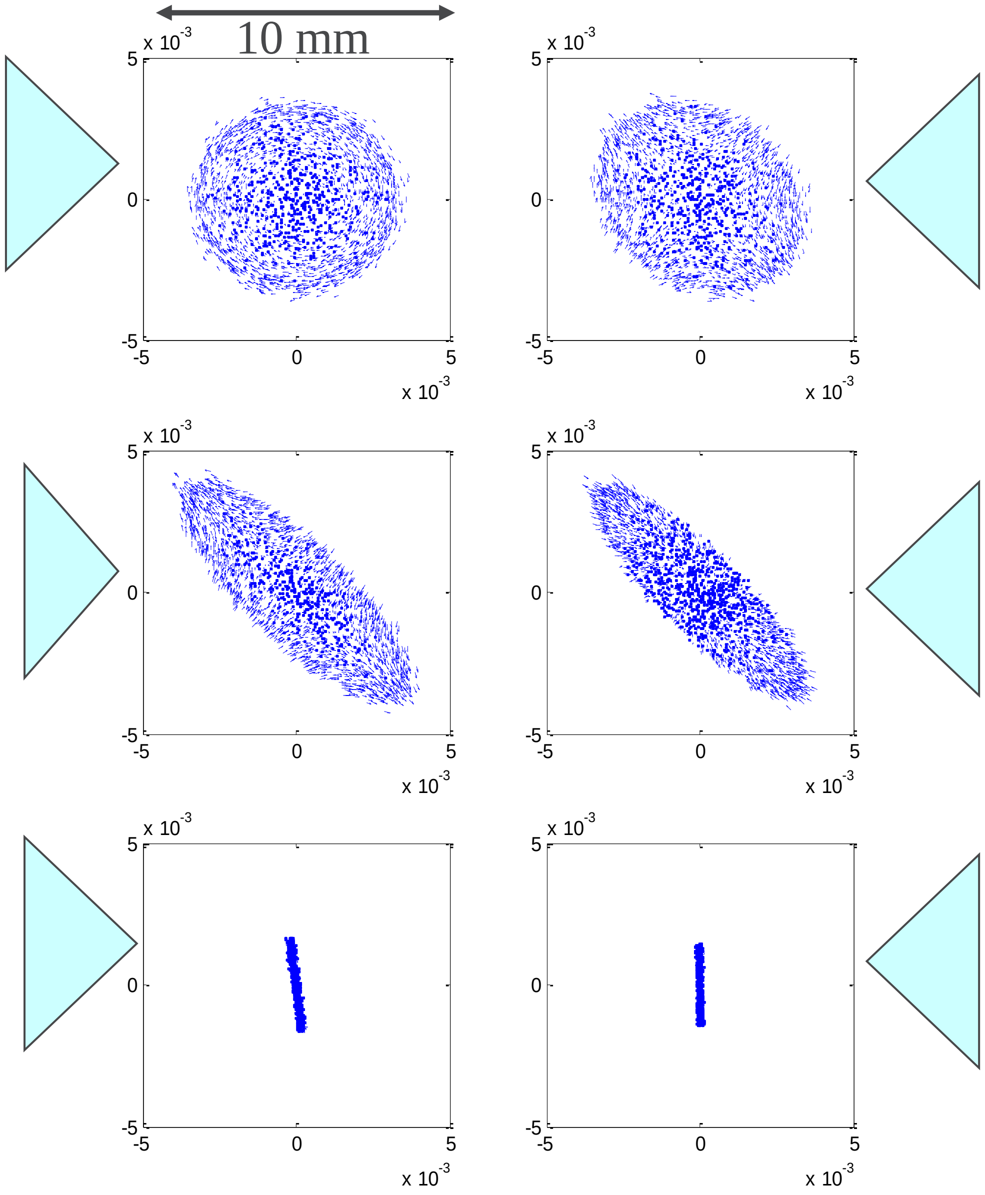

Right before 1st quad

Right after 1st quad

Right before 2nd Quad

Right after 2nd Quad

Right before 3rd quad

Right after 3rd quad

Removal of angular momentum and generating a flat beam

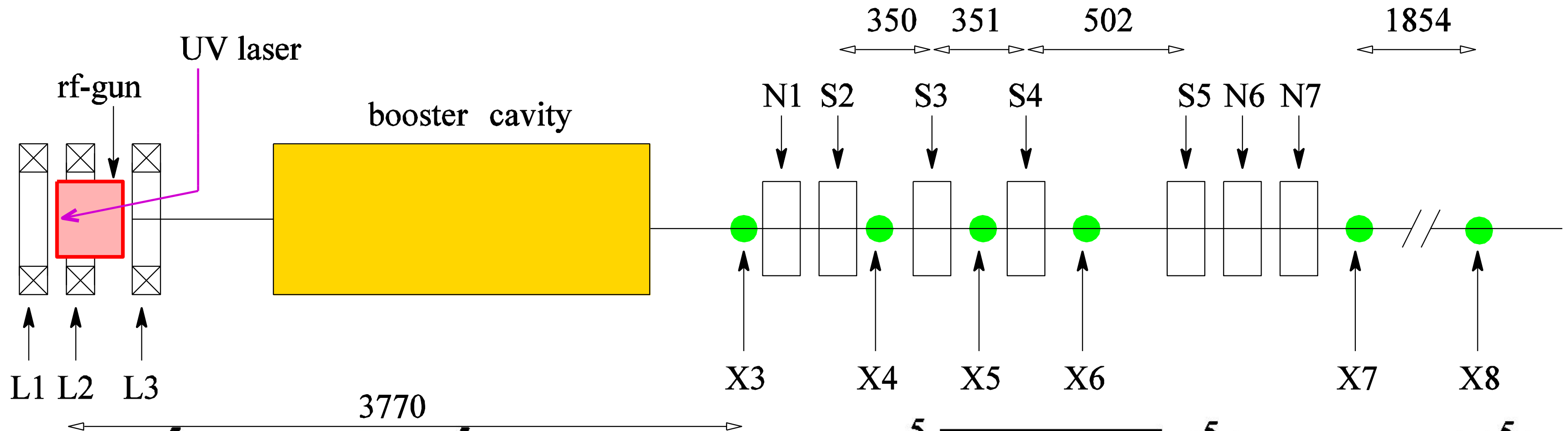

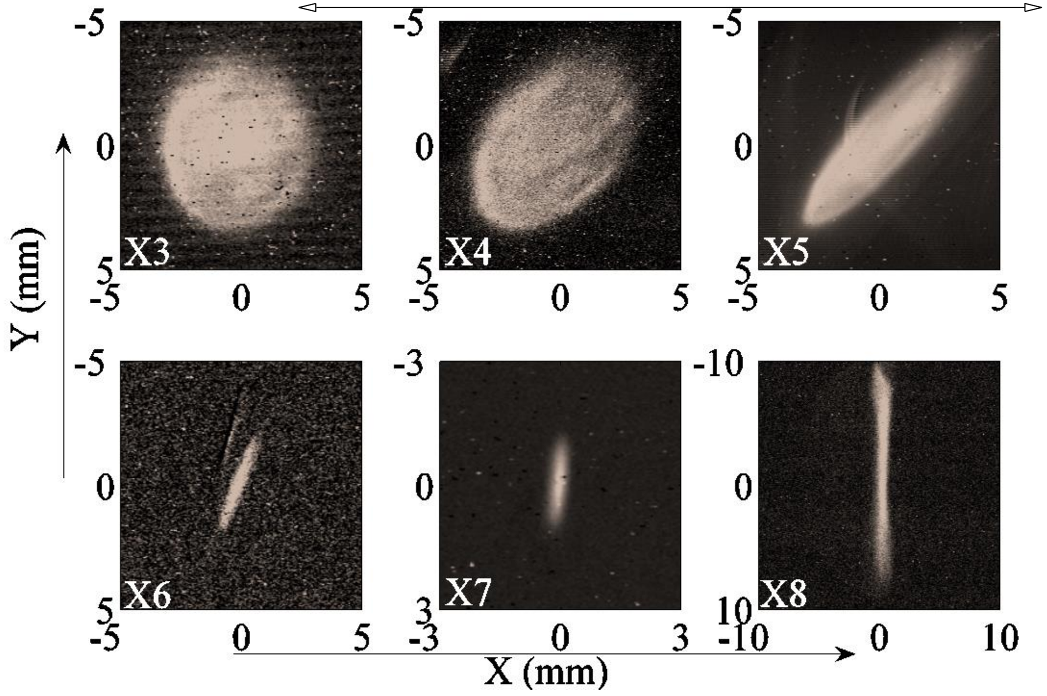

experiment

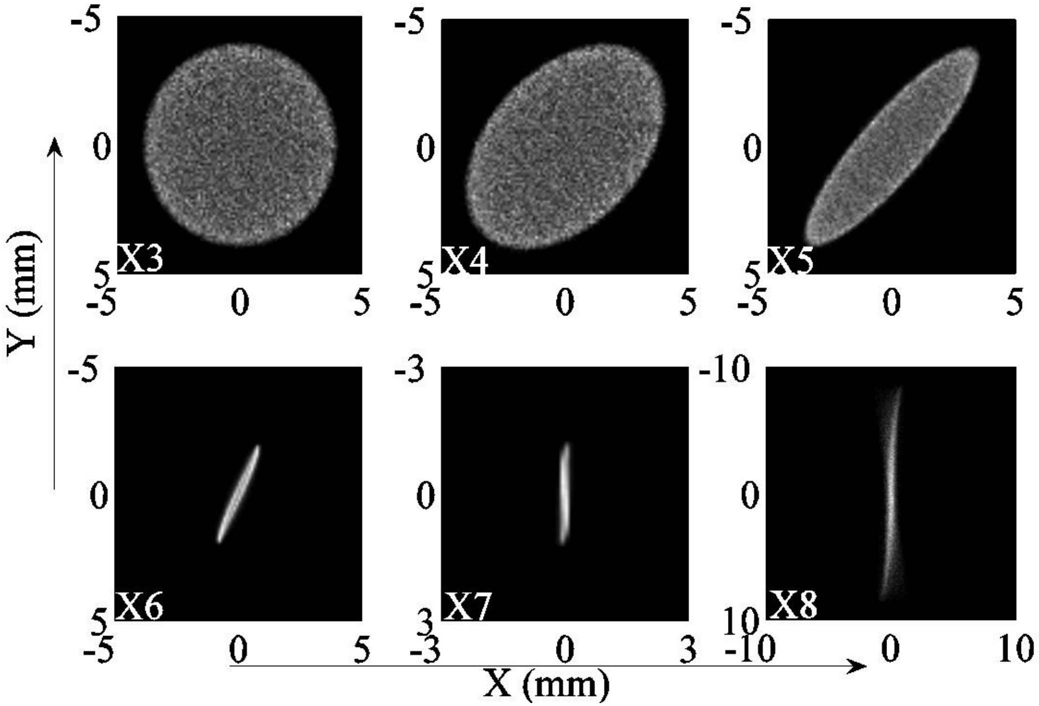

simulation

Single Slit Emittance Measurement Method

Blue: flat beam at X7; green: H or V slit inserted at X7; red: slit image at X8.

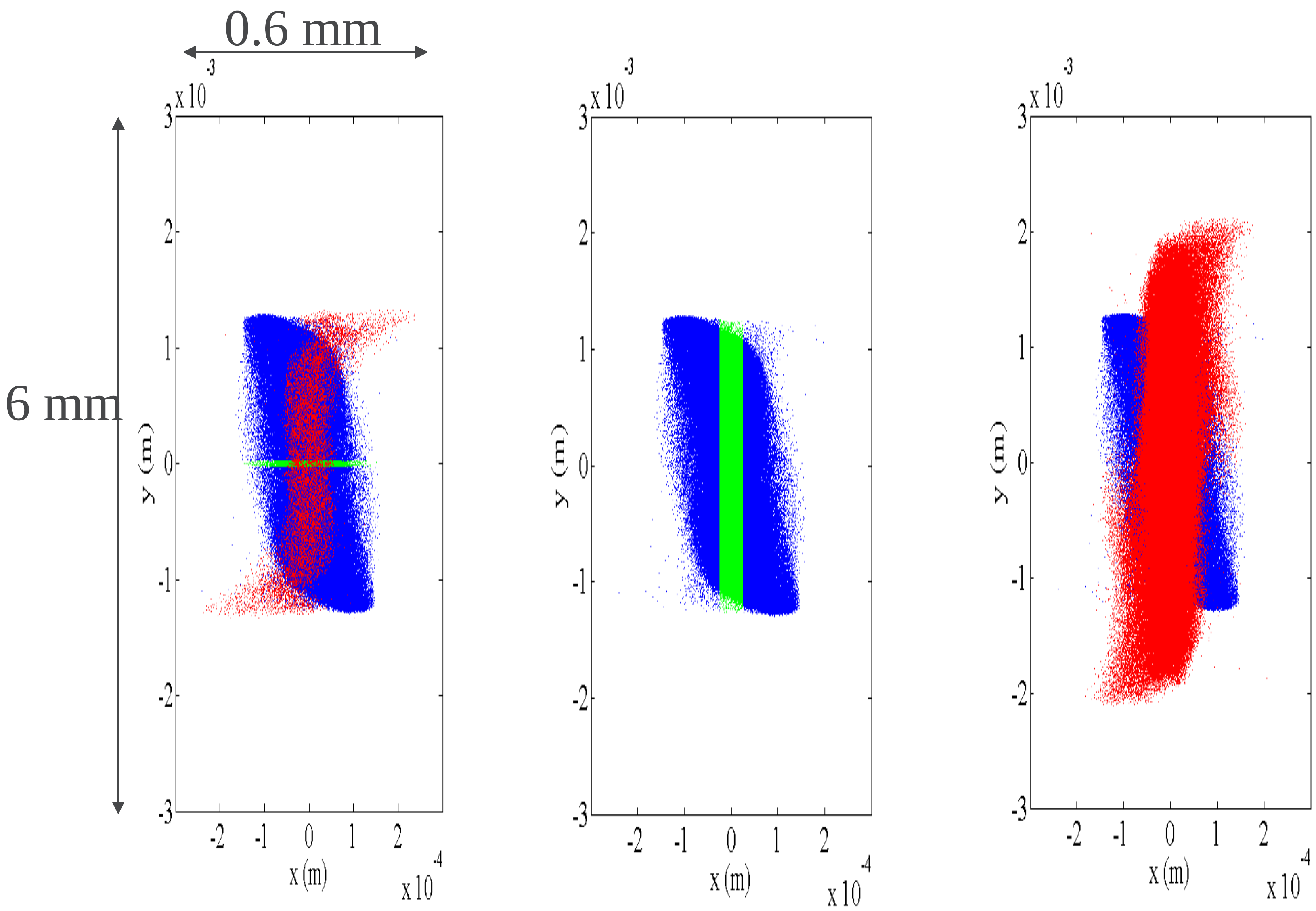

Flat-beam Emittance Measurements Using Slits: measurements and simulation

Solenoid setting:
main=190A, buck=0A,
secondary=75A

Laser σ = 0.76 mm
σ_t = 3 ps

E = 15.8 MeV
Q = 0.50 ± 0.05 nC

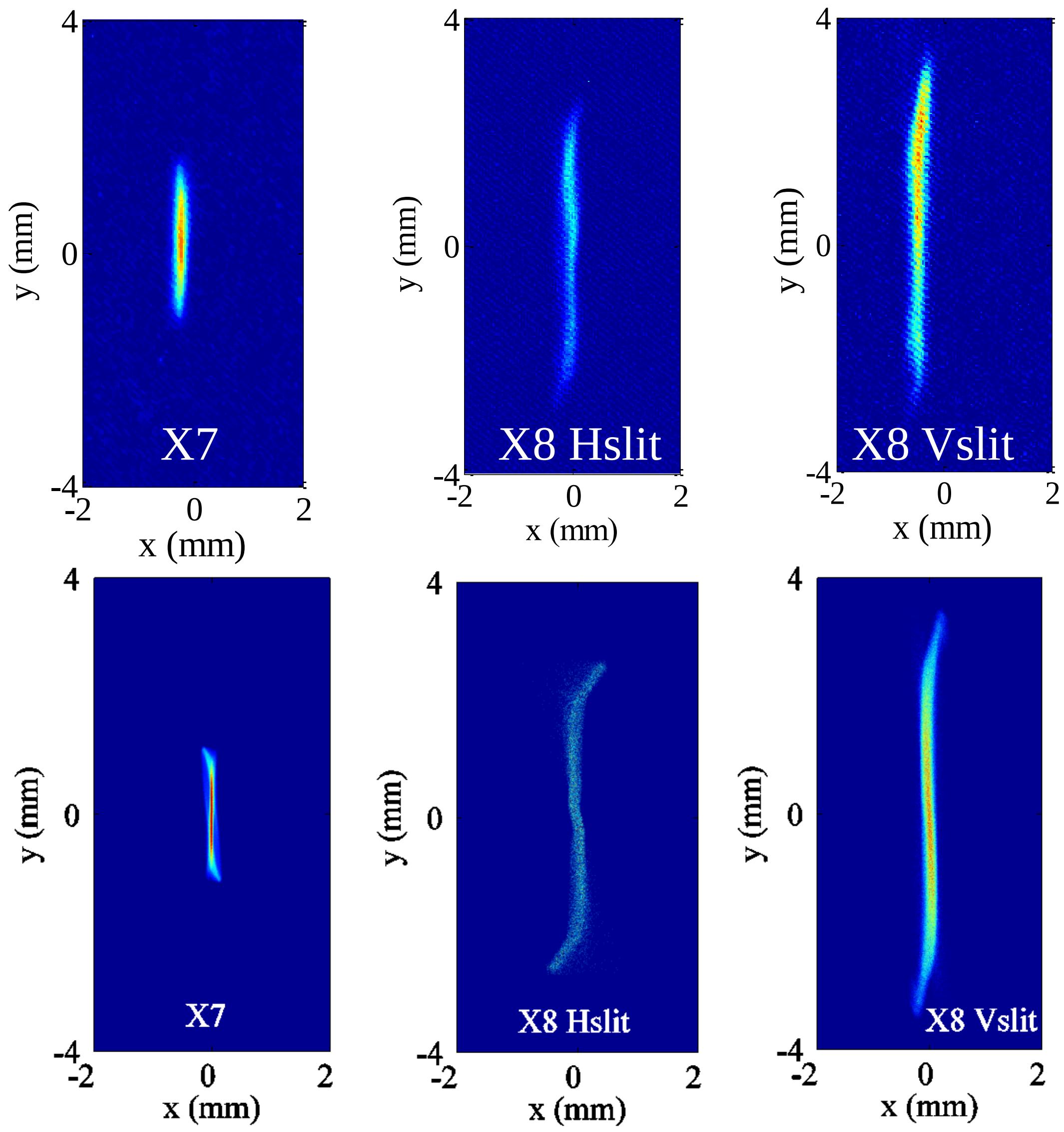

An Example of Flat Beam Generation

Solenoid setting: main=195A, buck=0A, secondary=75A

$\sigma = 0.97$ mm, $\sigma_t = 3$ ps

E = 15.86 MeV   Q = 0.51 ± 0.17 nC

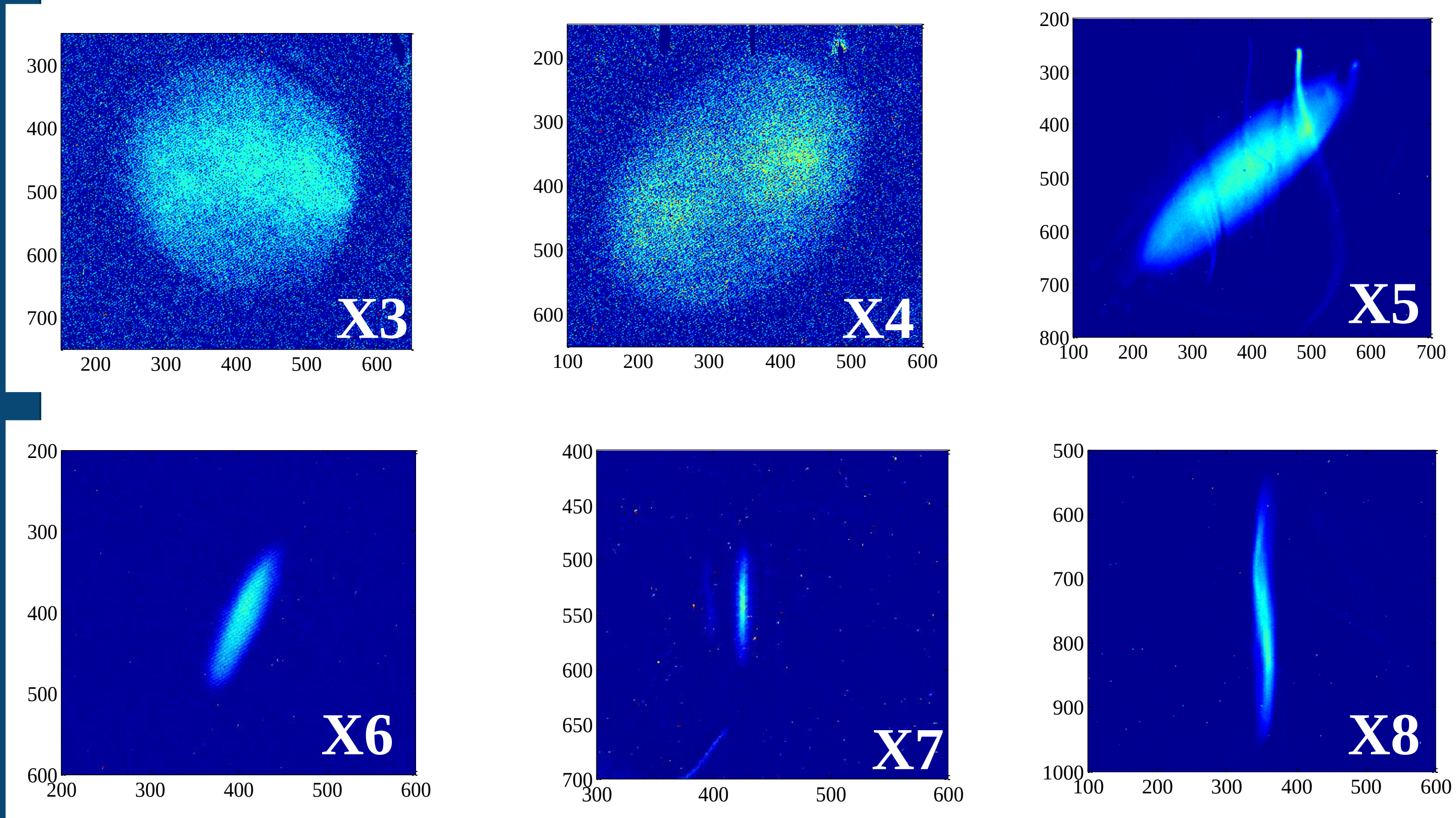

Photos of the beam taken along the beamline

ASTRA Simulation of the experiment

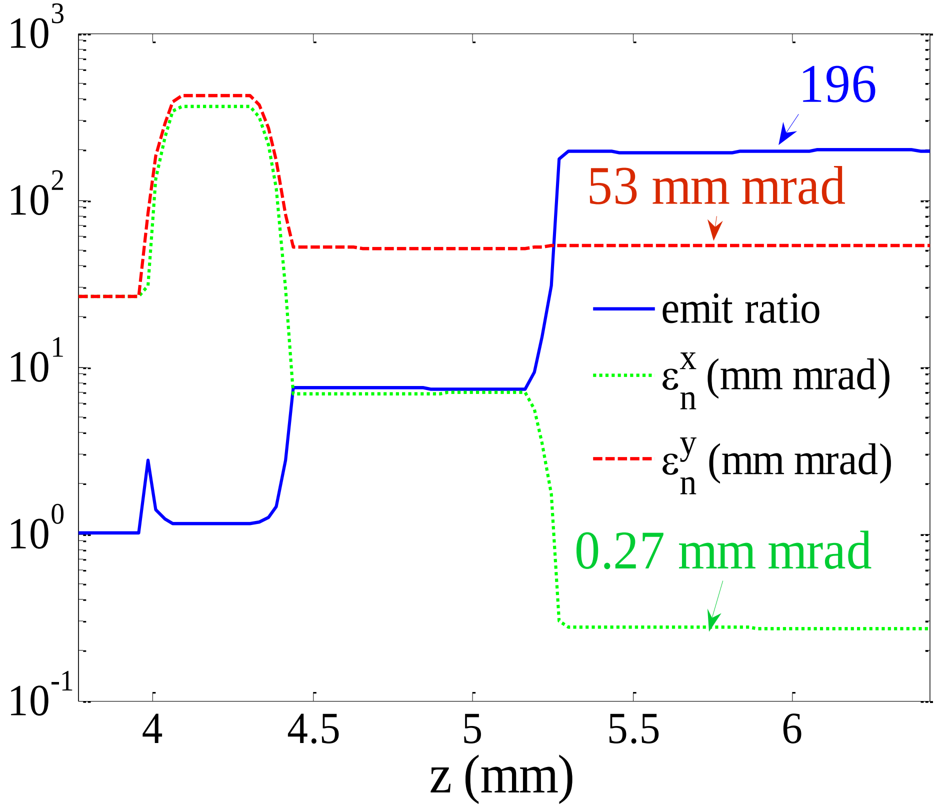

Phase-space exchange between two transverse planes

- The X-Y 4D phase space exchange is interesting for the next generation synchrotron radiation rings since it can lead to better horizontal injection efficiency. It has other applications as well.
- The X-Y phase space exchange can be accomplished using five skew quadrupoles to form the following transformation matrix:

$$R_{XY} = \begin{pmatrix} 0 & A \\ B & 0 \end{pmatrix}, \quad \begin{pmatrix} \mathbf{X} \\ \mathbf{Y} \end{pmatrix} \rightarrow R_{XY} \begin{pmatrix} \mathbf{X} \\ \mathbf{Y} \end{pmatrix} = \begin{pmatrix} A\mathbf{Y} \\ B\mathbf{X} \end{pmatrix}$$

$$R_{XY} = R_{\pi/4}{}^{-1} Q_1 L_1 Q_2 L_2 Q_3 L_2 Q_2 L_1 Q_1 R_{\pi/4}.$$

- Upon proper choice of quad strength and drift distance, the transformation matrix is given by: Where d_T is the total drift distance of the 5-quads Beamline.

$$R_{XY} = \begin{pmatrix} 0 & 0 & 1 & d_T \\ 0 & 0 & 0 & 1 \\ 1 & d_T & 0 & 0 \\ 0 & 1 & 0 & 0 \end{pmatrix}$$

Kim, K.-J., 2020, “Simple formula to determine the parameters of XY emittance exchange,” Argonne National Laboratory Technical Report No. ANL/APS/LS-365.

Emittance EXchange

Transverse-to-Longitudinal Phase-Space Exchange

- EEX therory:
  - 2002: Cornacchia and Emma, PRSTAB 5, 084001.
    - Partial exchange : chicane
  - 2006: Kim, AIP Conf. Proc. No. 821.
    - Complete exchange: double-dogleg
- 2010: Double-dogleg EEX experiment demonstration:
  - J. Ruan et al., PRL 106, 244801 (2011).
- 2010: Applications of EEX in beam current profile modulation:
  - Y. Sun et al., PRL 105, 234801 (2010).
  - G. Ha et al., PRSTAB 19, 121301 (2016).
  - G. Ha, et al., 2017, PRL 118, 104801 (2017).
- Double Emittance Exchange (DEEX)
  - A. Zholents et al., ANL/APS/LS-327 (2011).

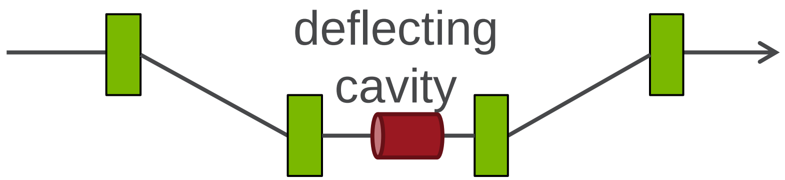

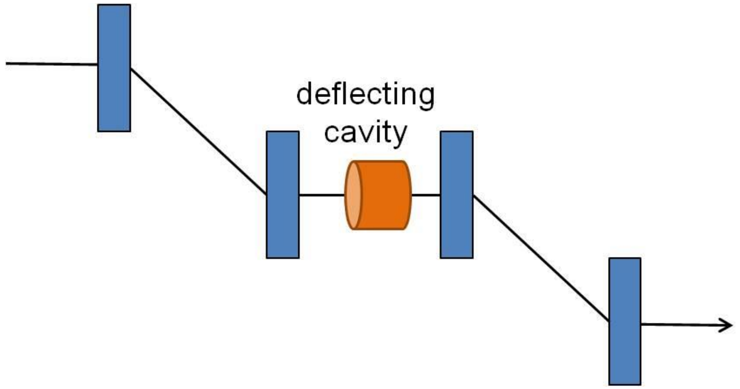

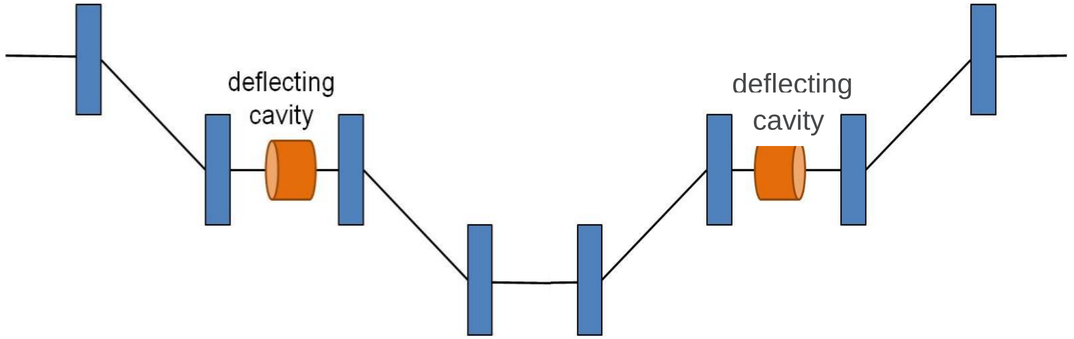

Transverse-to-Longitudinal Emittance EXchange

- Four dipoles + one deflecting cavity:
- Under thin-lens approximation, with proper matching of the deflecting cavity strength (k) and the dogleg dispersion (D), i.e., 1+kD=0, the diagonal sub-block elements of the exchanger's transfer matrix are zero ↔ the initial horizontal phase space is mapped into the longitudinal phase space, vice versa.
- With finite cavity length included, there will be non-zero terms in the diagonal blocks – which can be corrected by adding accelerating cells on the defecting cavity [1], or reduced by adjusting initial beam transverse and longitudinal phase space correlations.

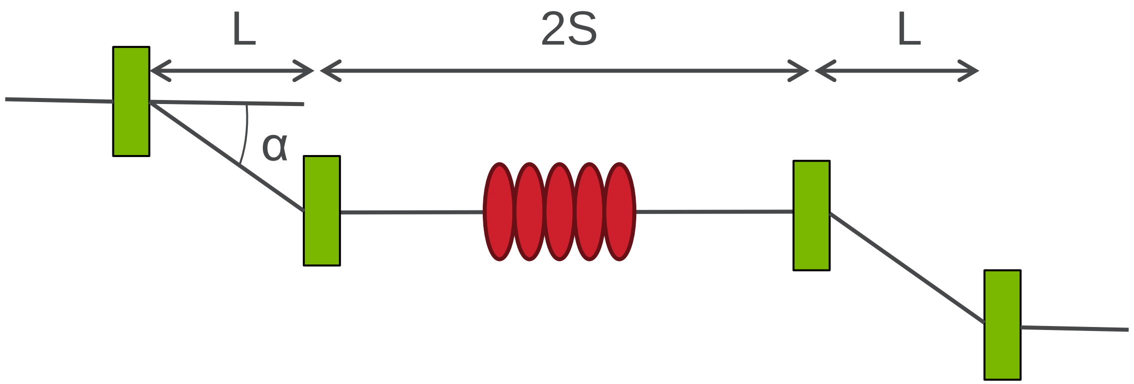

$$\begin{pmatrix} x \\ x' \\ z \\ \delta \end{pmatrix}_{out} = \begin{pmatrix} 0 & 0 & \frac{L+S}{\alpha L} & \alpha S \\ 0 & 0 & \frac{1}{\alpha L} & \alpha \\ \alpha & \alpha S & 0 & 0 \\ \frac{1}{\alpha L} & \frac{L+S}{\alpha L} & 0 & 0 \end{pmatrix} \begin{pmatrix} x \\ x' \\ z \\ \delta \end{pmatrix}_{in}$$

1] A. Zholents, ANL/APS/LS-327, May 2011

EEX beamline at A0 photoinjector, Fermilab

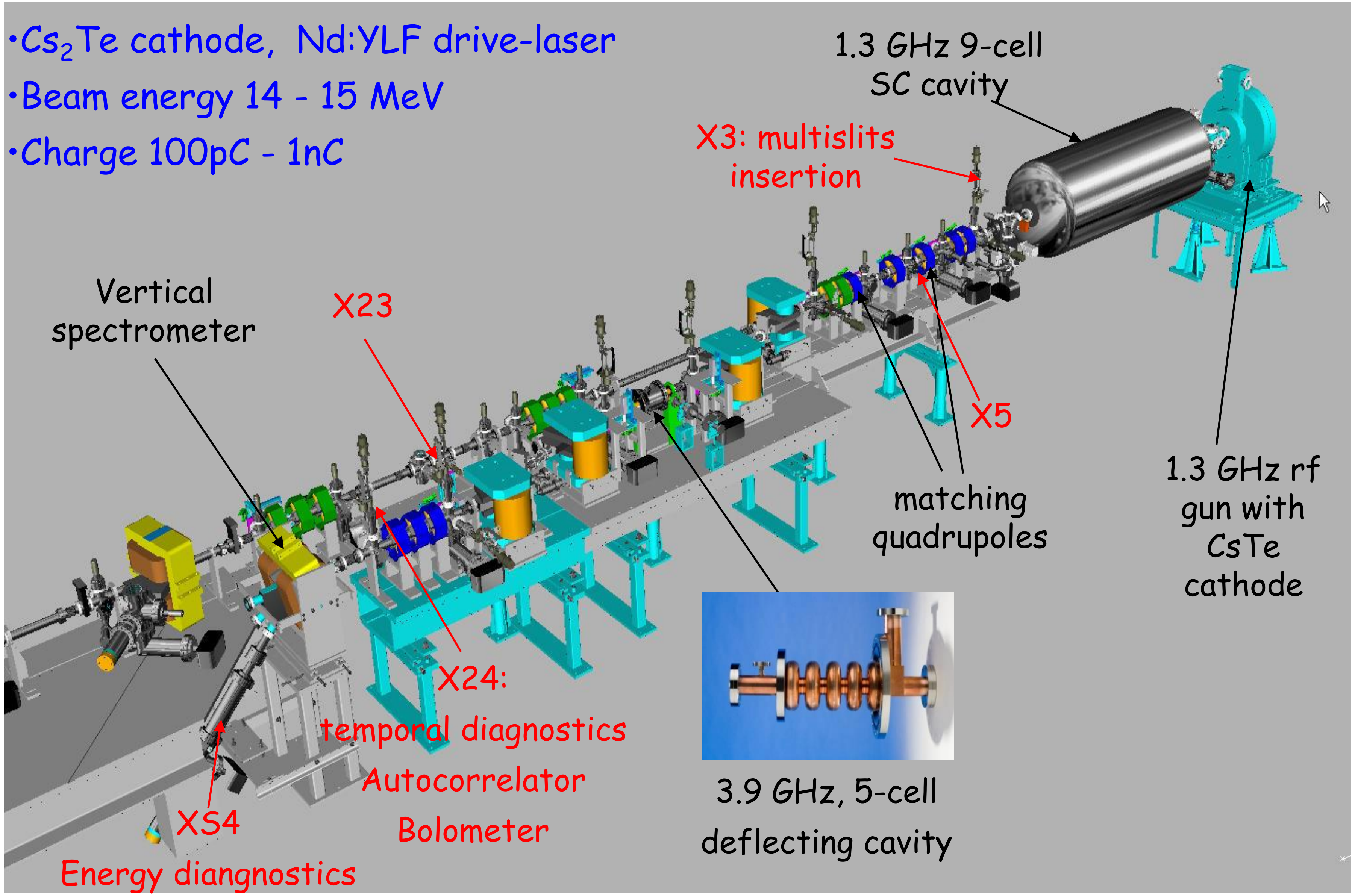

A0 EEX experiment and simulation at low charge

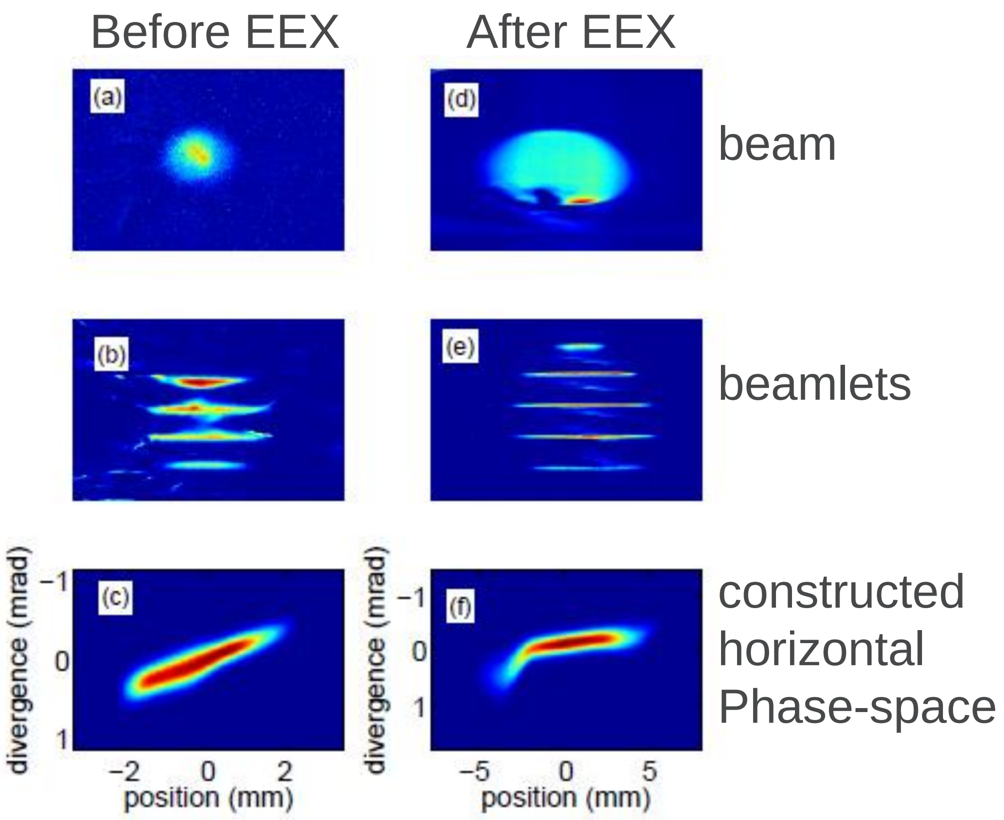

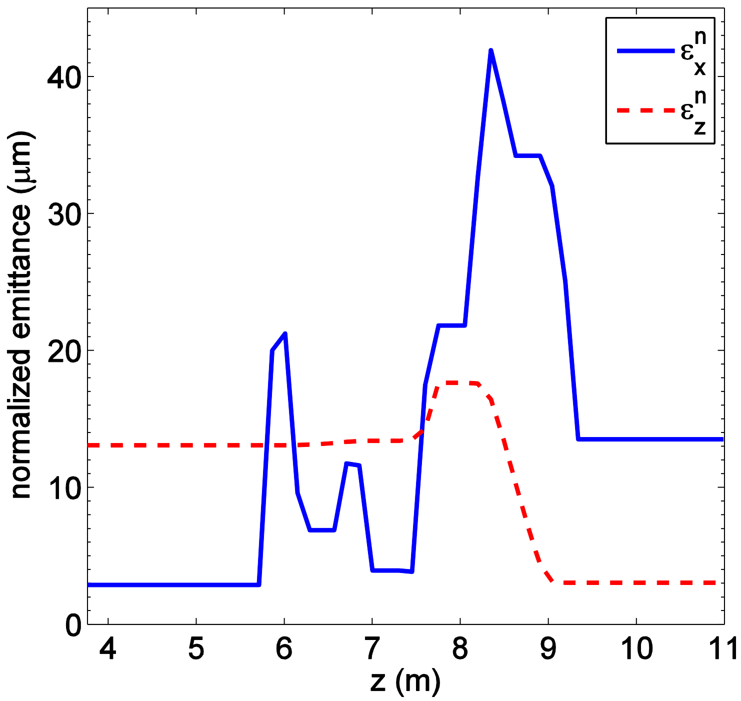

Norm. Emit.	Before EEX (exp.)	After EEX (exp.)	After EEX (simu.)
ε_x^n (μm)	2.9±0.1	11.3±1.1	13.5
ε_z^n (μm)	13.1±1.3	3.1±0.3	2.9
ε_y^n (μm)	2.4±0.1	2.9±0.5	3.0

Thick-lens Effect

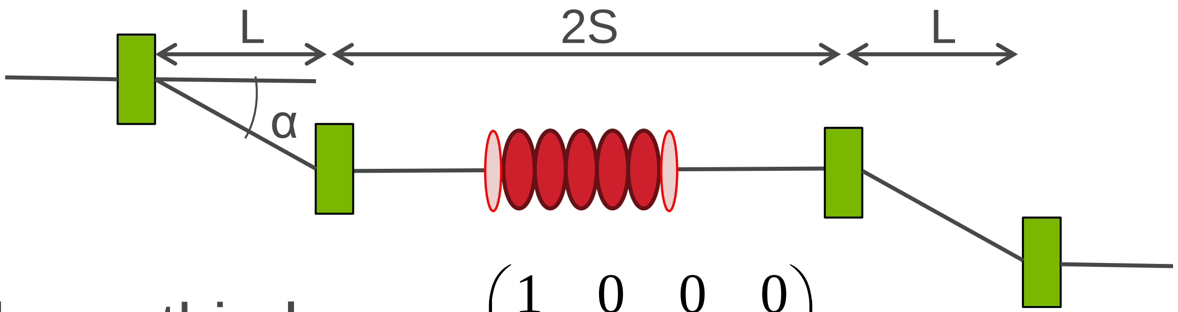

So far, only thin-lens approximation is considered for the transfer matrix of the deflecting cavity.

$$\begin{pmatrix} 1 & 0 & 0 & 0 \\ 0 & 1 & k & 0 \\ 0 & 0 & 1 & 0 \\ k & 0 & 0 & 1 \end{pmatrix}$$

When taking into account of the finite cavity length *l*, the matrix is

$$\begin{pmatrix} 1 & l & kl/2 & 0 \\ 0 & 1 & k & 0 \\ 0 & 0 & 1 & 0 \\ k & kl/2 & k^2 l/6 & 1 \end{pmatrix}$$

The R_{43} leads to non-vanishing terms in the diagonal blocks of the EEX matrix.

Adding accelerating cavity to the deflecting cavity solves the problem.

(A. Zholents, ANL/APS/LS-327, May 2011)

Longitudinal Phase Space Manipulation via EEX
-- bunch train generation

Longitudinal Shaping using EEX: sub-ps Bunch Train Generation

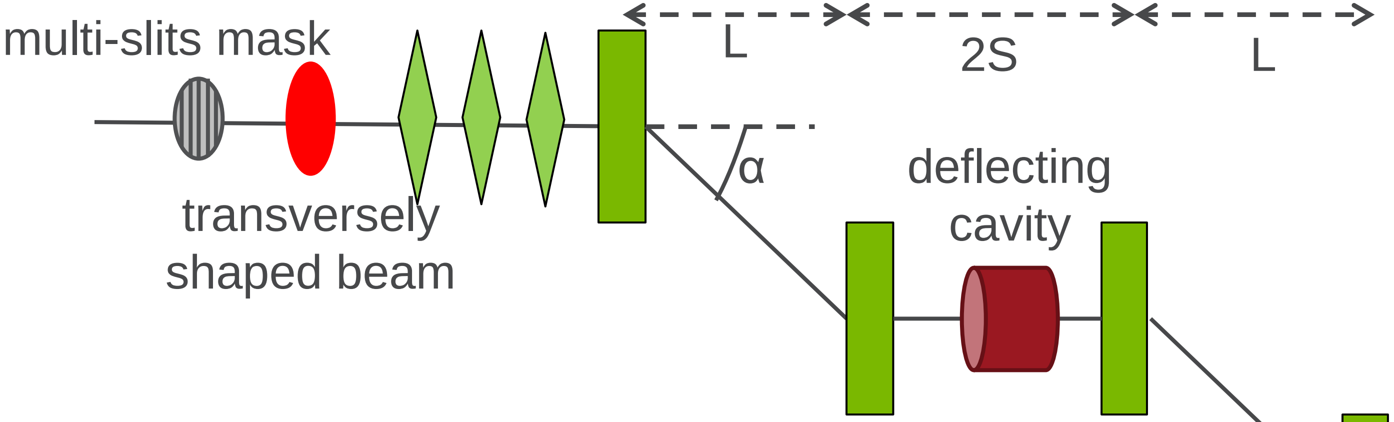

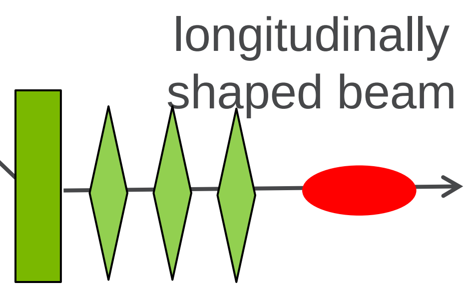

Inserting multi-slits mask into the beamline, the horizontal beam profile is sliced into several beamlets.

After the Phase-space Exchange (PEX), horizontal and longitudinal phase-space are swapped. Therefore, beam is now a bunch-train.

$$\begin{bmatrix} 0 & 0 & \frac{L+S}{L\alpha} & S\alpha \\ 0 & 0 & \frac{1}{L\alpha} & \alpha \\ \alpha & S\alpha & 0 & 0 \\ \frac{1}{L\alpha} & \frac{L+S}{L\alpha} & 0 & 0 \end{bmatrix} \Rightarrow \begin{bmatrix} z_f \\ \delta_f \end{bmatrix} = \begin{bmatrix} \alpha & S\alpha \\ \frac{1}{L\alpha} & \frac{L+S}{L\alpha} \end{bmatrix} \begin{bmatrix} x_i \\ x_i' \end{bmatrix}$$

Quadrupole channels before and after EEX to minimize the contribution from x_i'.

Final bunch length control via initial horizontal beam focusing

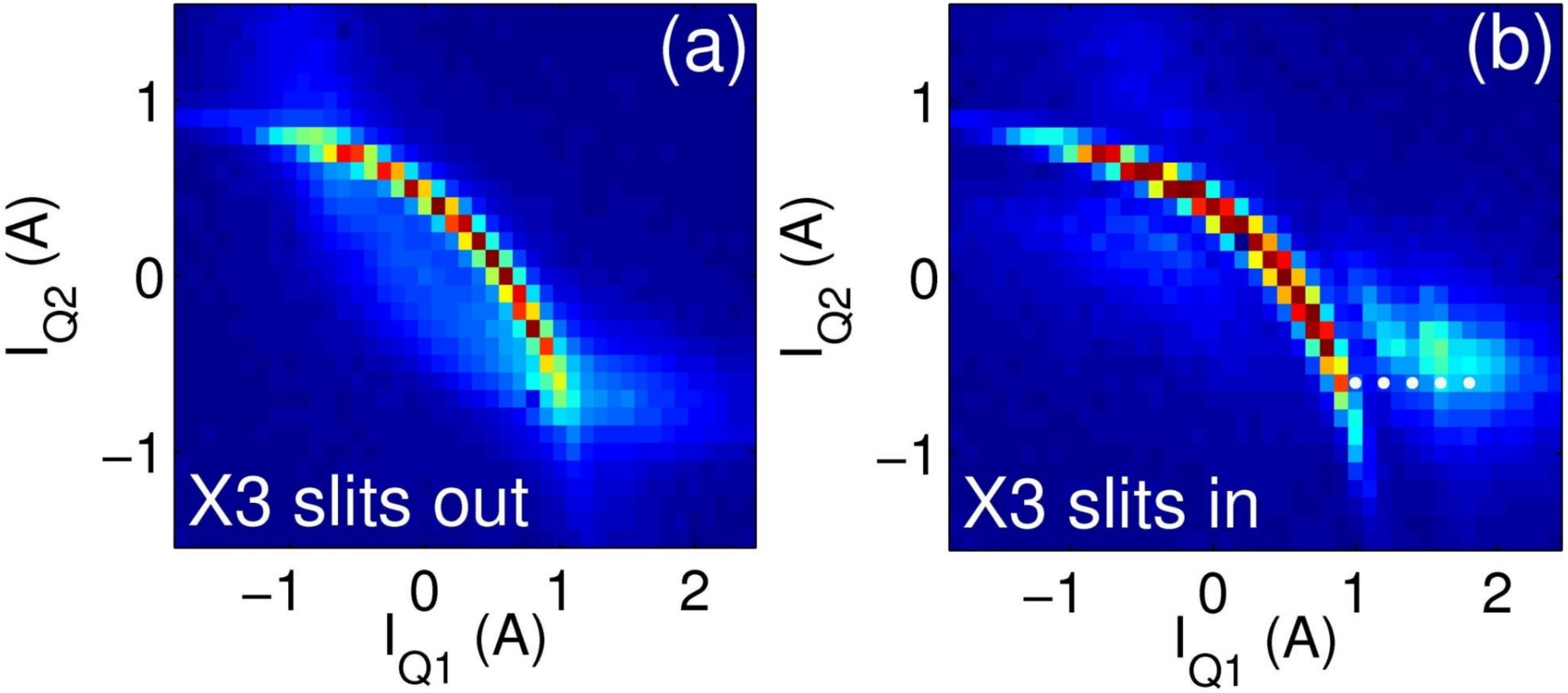

The final beam longitudinal properties can be controlled by initial horizontal beam parameters. While scanning the currents of two quadrupoles upstream of the double-dogleg beamline, the final bunch length after EEX can be monitored using an auto-correlator + bolometer system. Fig. (a) shows such a quadrupole scan without slits inserted, and (b) with the slits. The small island appeared with the slits inserted is related to the coherent radiation from the bunch-train.

Experimental demonstration of the sub-ps bunch train: energy domain

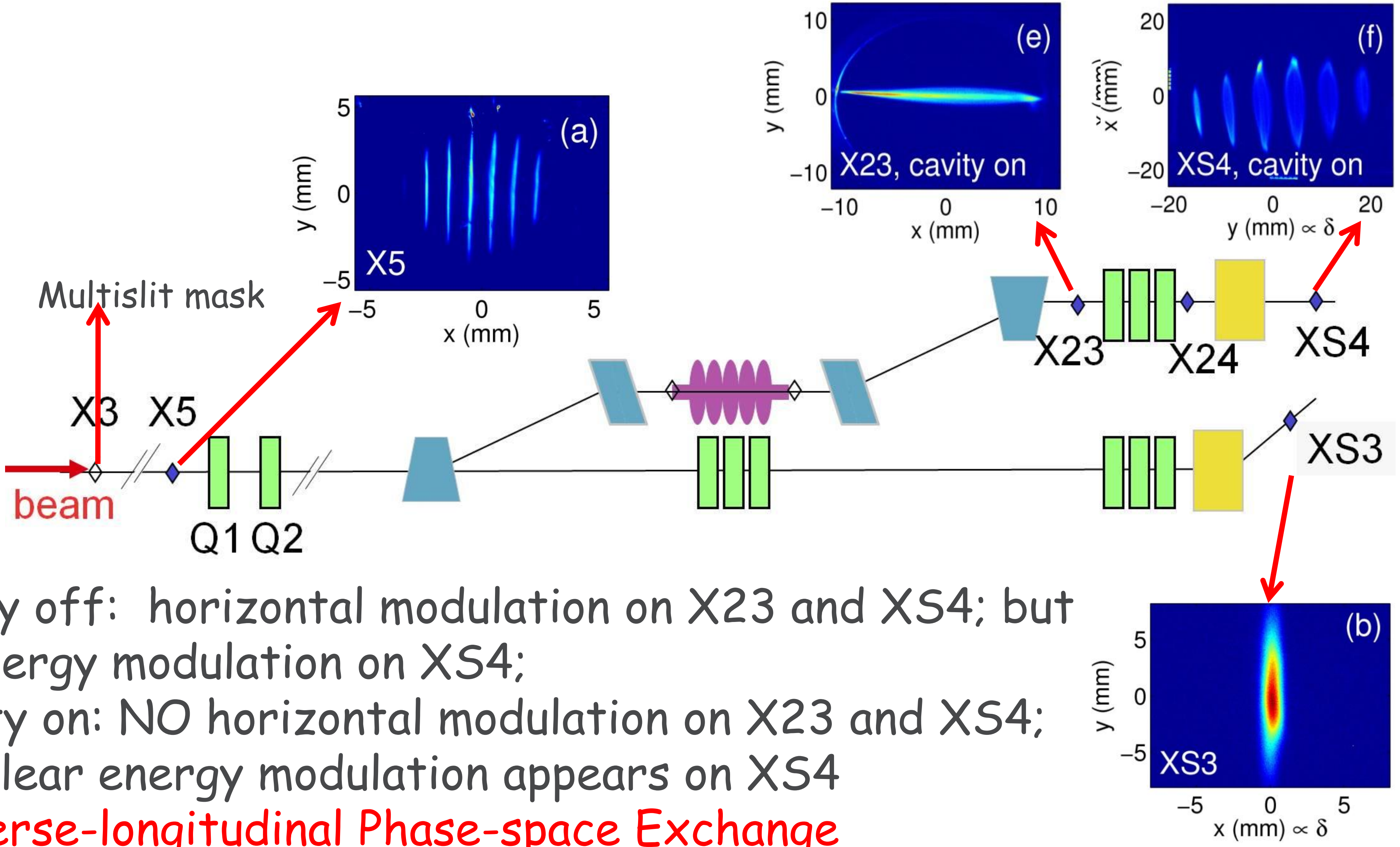

(1)cavity off: horizontal modulation on X23 and XS4; but no energy modulation on XS4;

(2)cavity on: NO horizontal modulation on X23 and XS4; but clear energy modulation appears on XS4

Transverse-longitudinal Phase-space Exchange

Experimental demonstration of the sub-ps bunch train: time domain

The bunch train temporal structure is measured via the CTR signal measured downstream of EEX.

A liquid-helium-cooled bolometer is used as the detector of the Michelson autocorrelator.

Multipeaks of the autocorrelation function are measured when the slit mask is inserted, compared to a single peak when the mask is out.

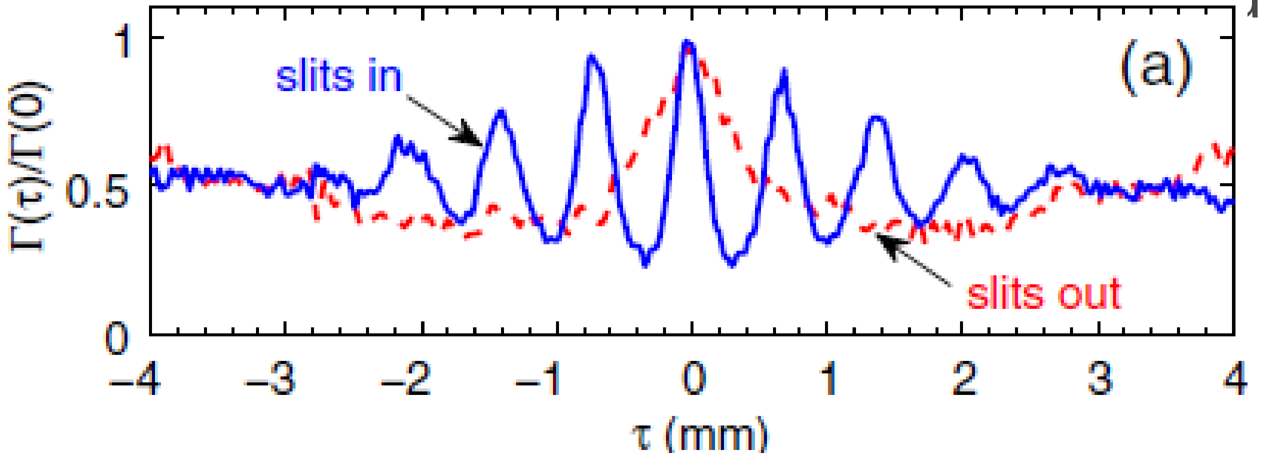

Experimental demonstration of the sub-ps bunch train

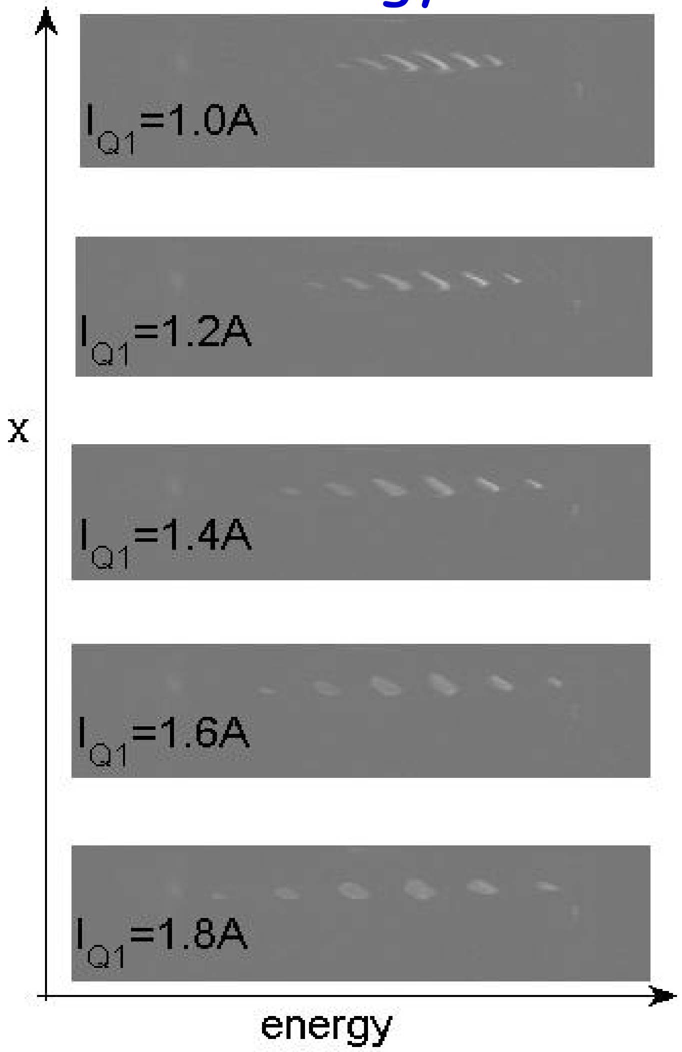

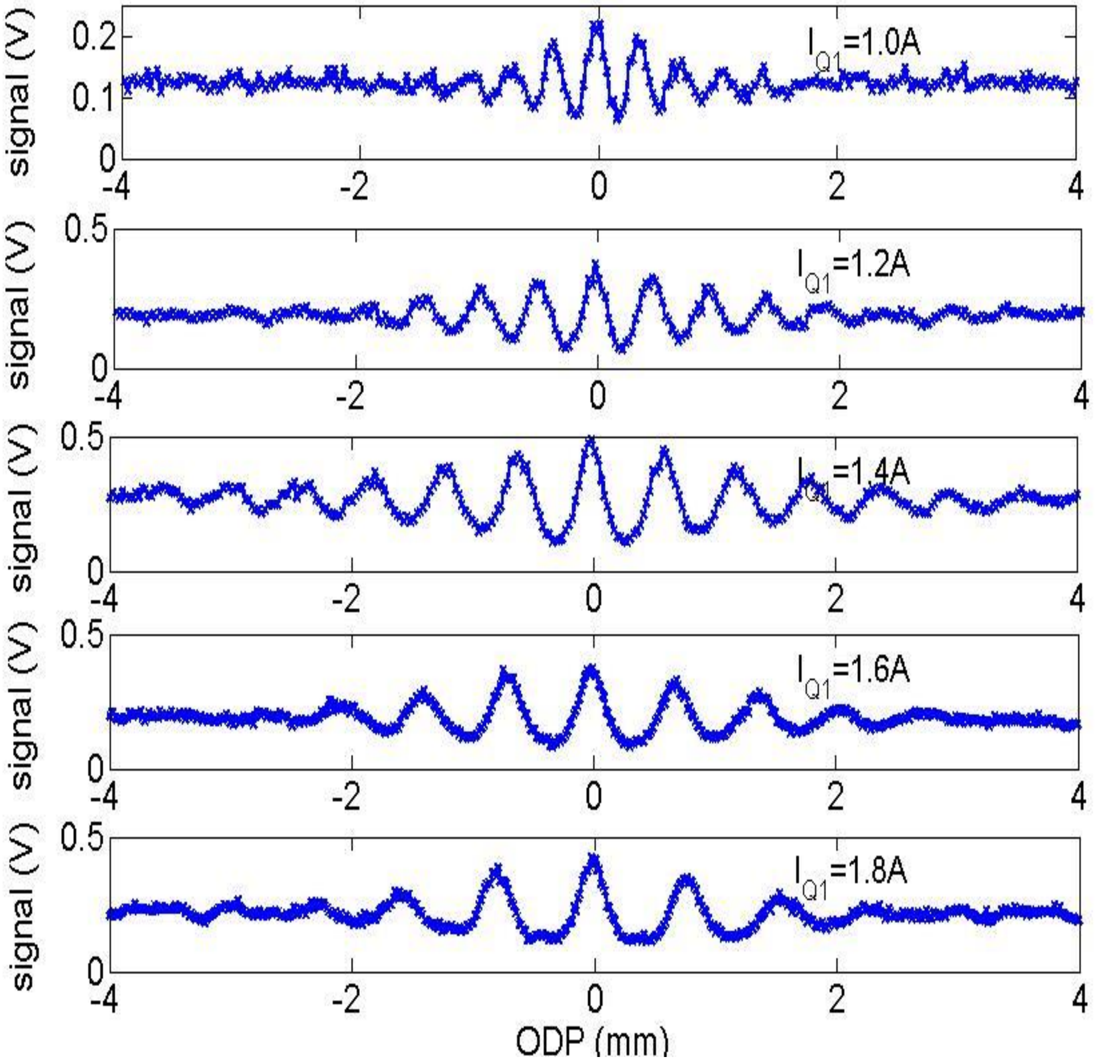

Y.-E Sun et al, PRL 105, 234801 (2010).

Experimental demonstration of the sub-ps bunch train: variable bunch separation

The bunch separation is extracted from the autocorrelation function to be [350 ~ 760] μm. The separation can be easily tuned by changing the currents of one single quadrupole upstream of EEX.

The corresponding CTR measured from these bunch trains is a narrow-band ($\delta f/f \approx 20\%$ at 0.5THz) with tunable frequency of [0.37 0.86] THz. *

Assuming Gaussian distribution, the minimum individual bunch rms duration measured is less than 300 fs.

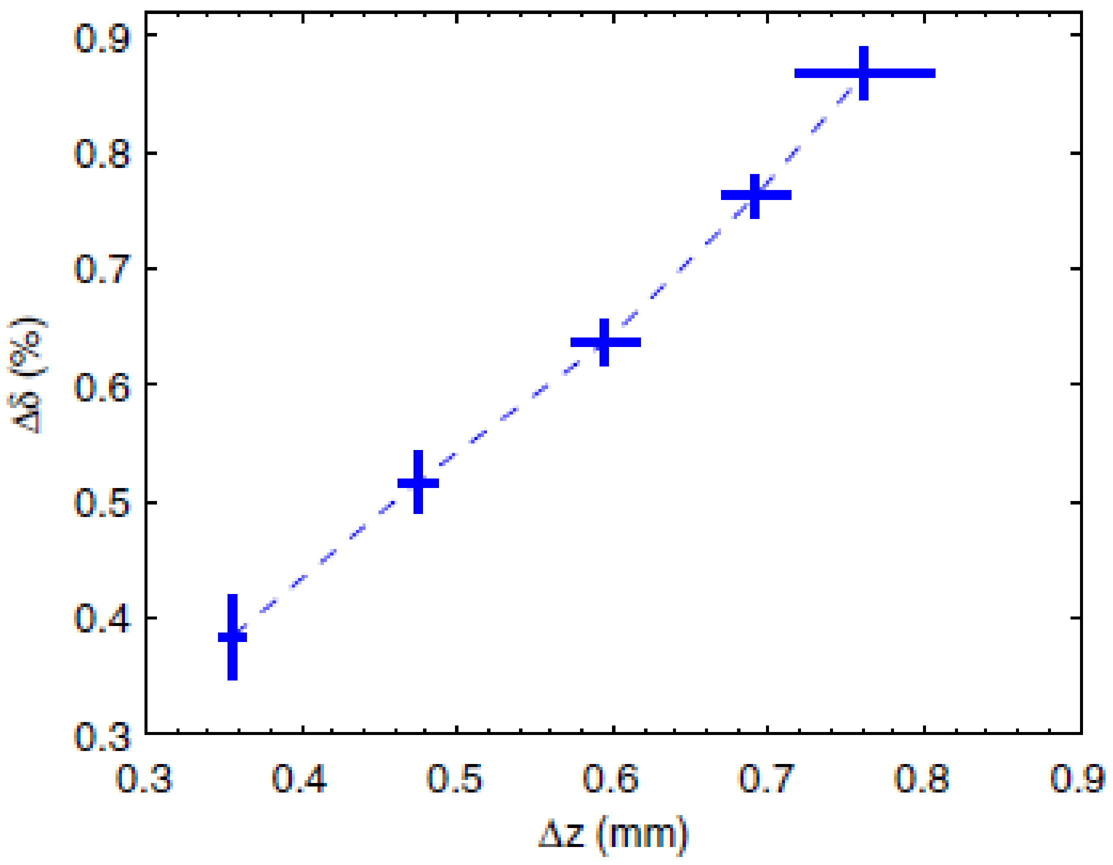

*P. Piot et al., Applied Physics Letters **98**, 261501 (2011)

Longitudinal Bunch Shaping via EEX -- Precise Beam Profile Control

Arbitrary Beam Longitudinal Beam Profile

- Transverse beam shaping is mature. Tools to obtain desired transverse beam profile include shaping the drive-laser transverse profile for a photo-injector, inserting masks in the beam path, using quadrupoles to focus/defocus etc.

- Longitudinal shaping techniques to achieve arbitrary beam profile are rather limited relative to transverse shaping.

- EEX offers an opportunity to shape the beam transversely and then convert it to longitudinal – recently demonstrated at the Argonne Wakefield Accelerator (AWA/ANL).

(Slide from J. Power, AAC2016)

Double dogleg EEX beam line at AWA

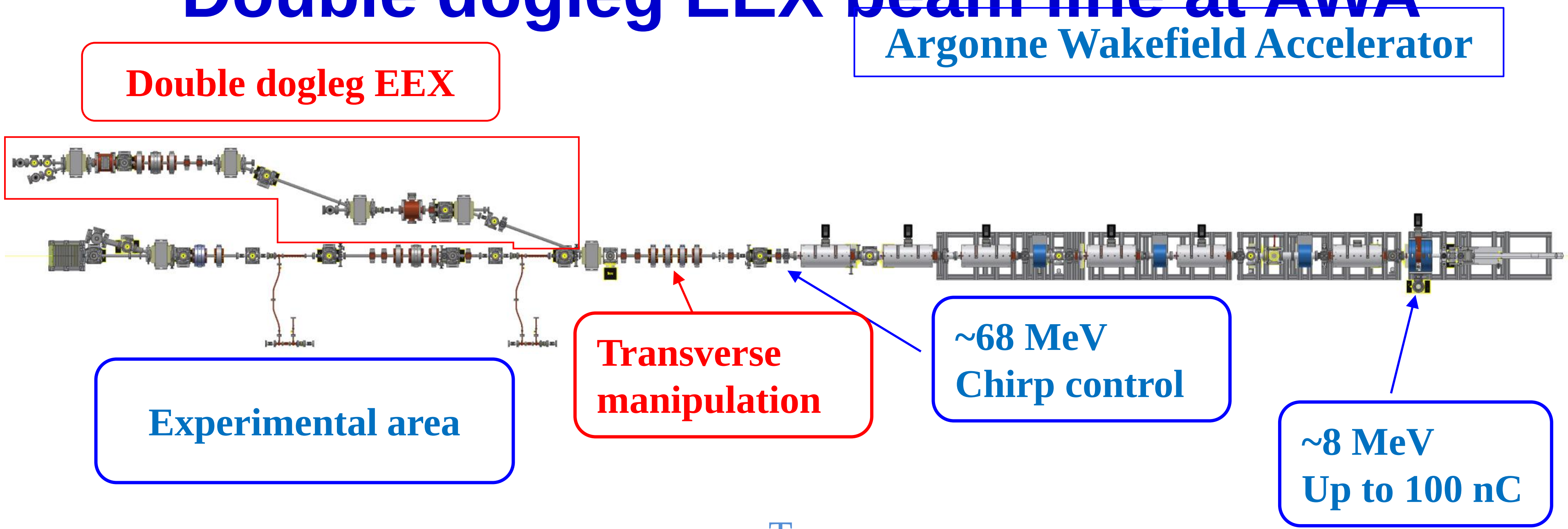

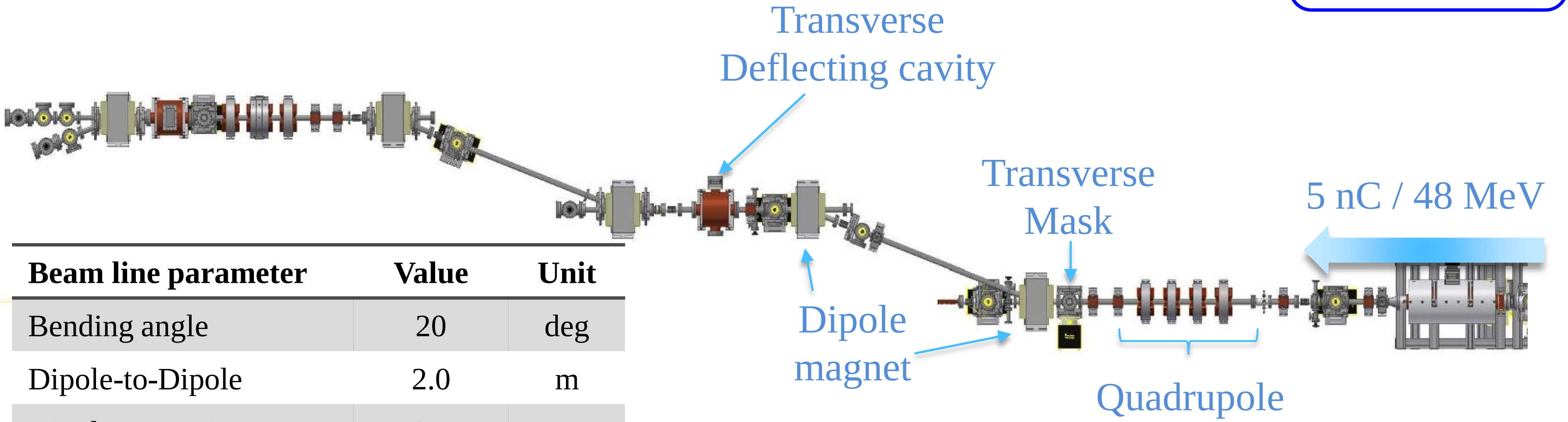

Beam line parameter	Value	Unit
Bending angle	20	deg
Dipole-to-Dipole	2.0	m
Dipole-to-TDC	0.5	m
Power to TDC	1.2	MW

Argonne NATIONAL LABORATORY

Demonstration of property exchange

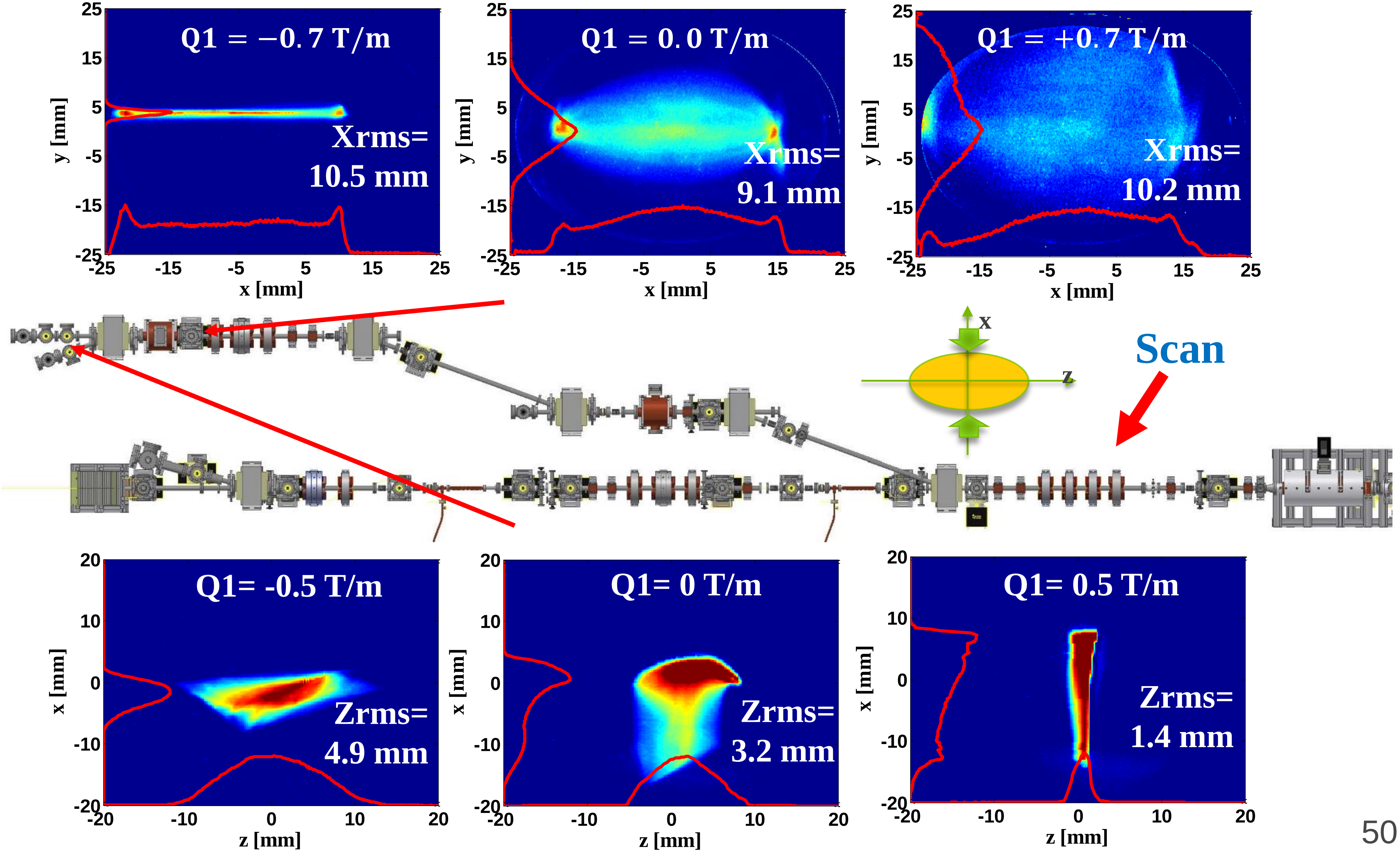

Argonne NATIONAL LABORATORY

(Slide from J. Power, AAC2016)

Demonstration of longitudinal bunch shaping at AWA/ANL

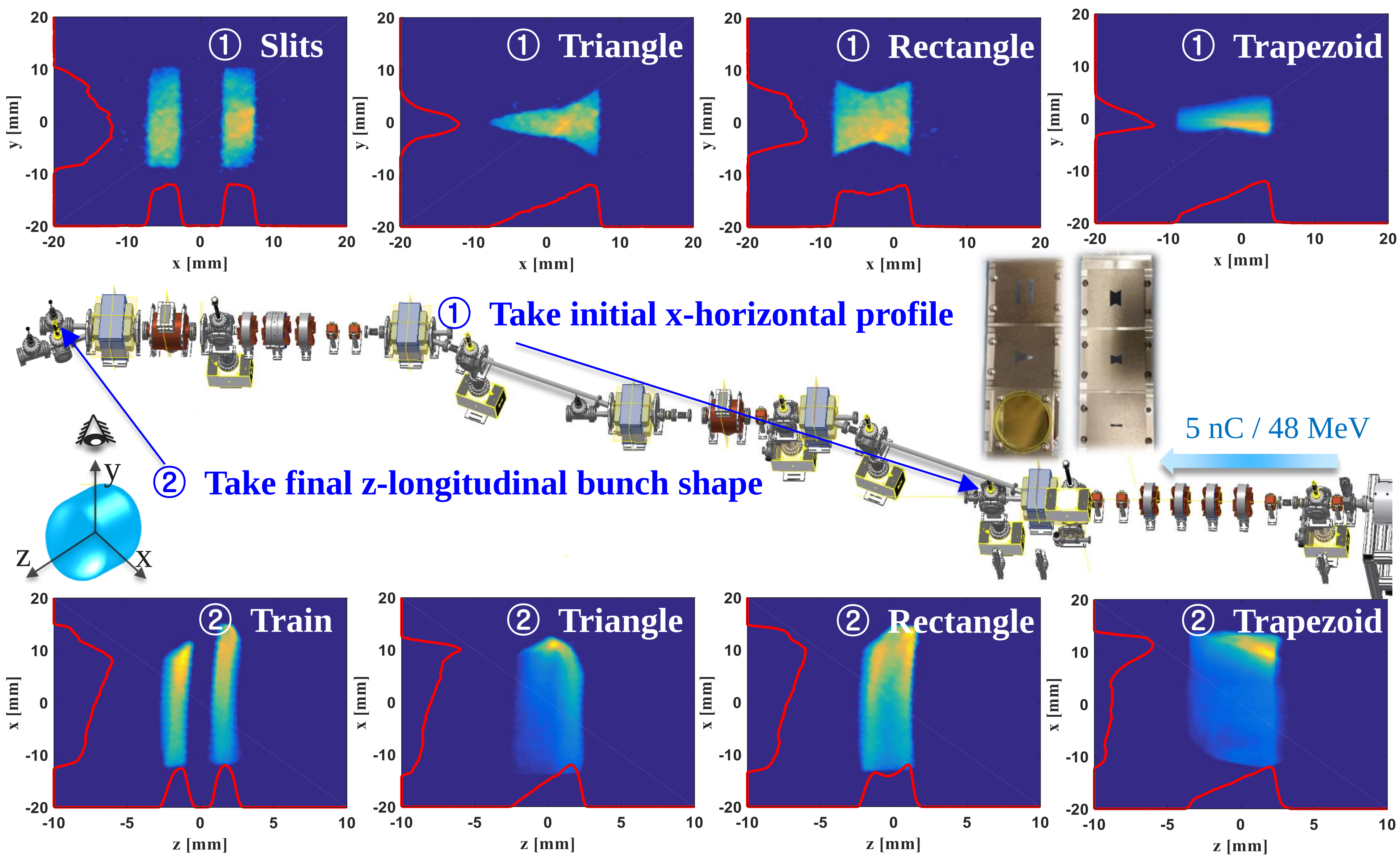

(Slide from J. Power, AAC2016)

Double Emittance EXchange

Single and Double Stage EEX

- So far we have worked with single stage EEX:
  - The double-dogleg EEX approach leave the beam line with a transverse offset, not desired in a straight linac accelerator tunnel;
  - As the transverse and longitudinal phase space exchange only once, the final transverse emittance might be larger than before the EEX – which may not be a desired feature for some applications.

- Double stage EEX*
  - Adding another double-dogleg EEX as a second stage will solve the two issues encountered above.
  - In between the two stages of EEX, mature transverse phase space manipulation techniques can be deployed to create final longitudinal phase space.

[*]A. Zholents et al., ANL/APS/LS-327 (2011)

Shaping via Double Emittance Exchange (DEEX)

- DEEX can be used as a way of tuning the final LPS correlation of the beam by properly designing the insertion beamline optical lattice between the two EEXs. The second EEX converts the transversely fine-tuned beam via the insertion beamline to the longitudinal phase space.

For example, bunch compression can be accomplished without any longitudinal phase-space chirp .

a) Schematic of a double-EEX-based bunch compressor with (b),(c) a simulated example of an application that provides a tenfold increase in modulation frequency of an incoming laser-modulated electron beam.

From Zholents and Zolotorev, 2011.

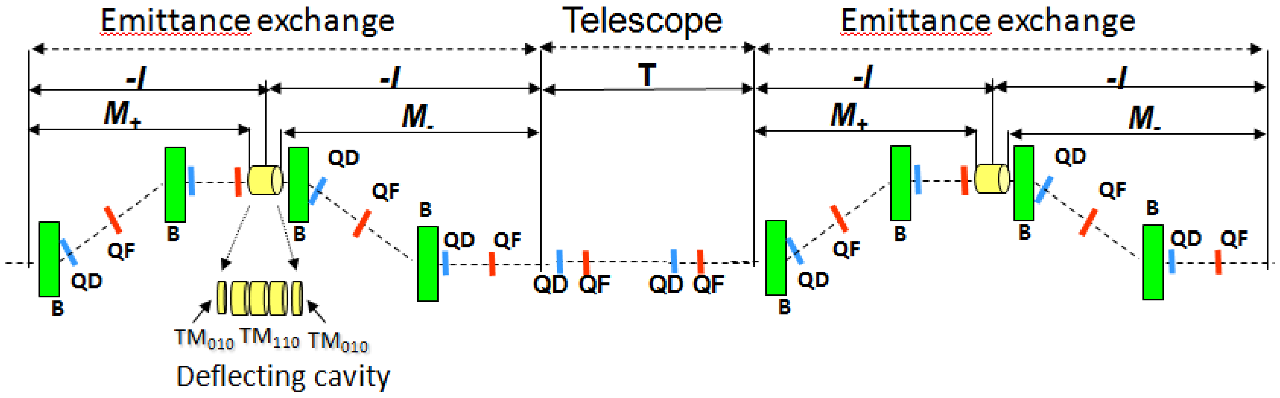

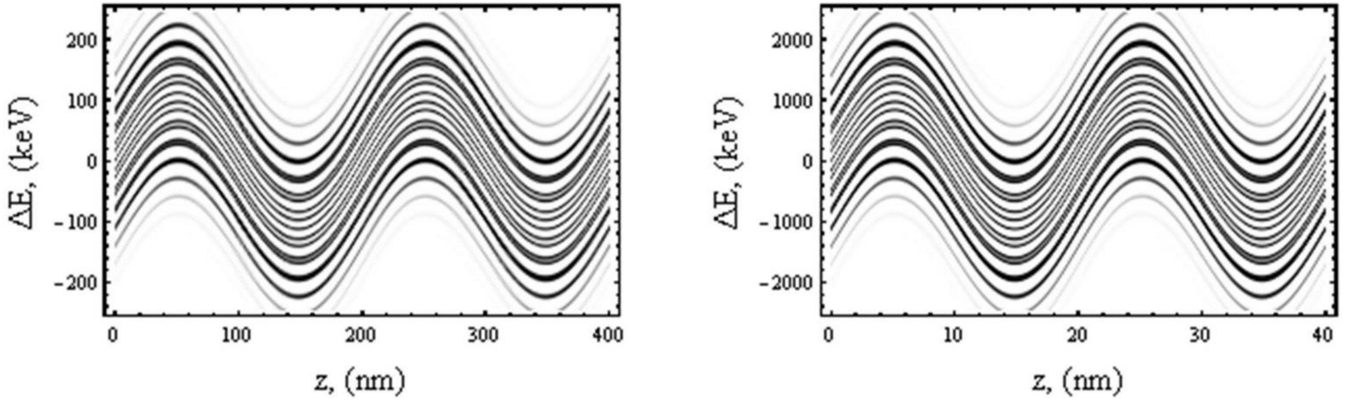

Shaping via Double Emittance Exchange (DEEX)

- DEEX enables control of nonlinear correlation in the longitudinal phase space using nonlinear magnets between the two EEXs.
- Beam final energy spread reduction via control of the longitudinal-phase-spacenonlinearities with a DEEX configuration.

A sextupole magnet located downstream of the first EEX, imposes a quadratic correlation.

Overview of a DEEX-based energy-spread reduction via correction on quadratic nonlinearity with a sextupole magnet.
From Seok, Ha et al., 2019.

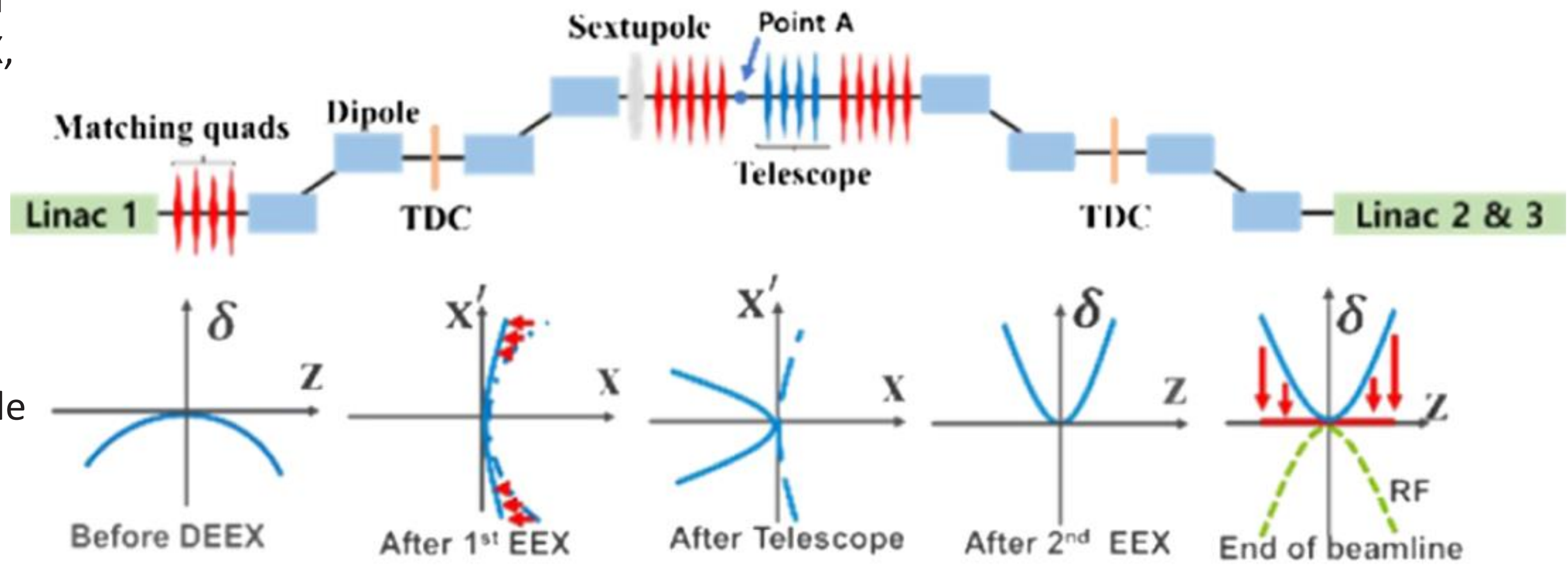

Shaping via Double Emittance Exchange (DEEX)

- A DEEX beamline combined with a phase-space modulator (e.g. a wakefield structure or transverse wiggler) can be used to generate density spikes on time and energy axes.

Example: a dielectric structure in front of a double-EEX beamline imprints a sinusoidal modulation on the longitudinal phase space→ then converted into energy spikes that are controlled with quadrupole magnets located in the middle of the DEEX. Because the EEX beamline provides control of R55, R56, R65, and R66, it can be used to generate a multienergy beam with controllable time separation from a single bunch.

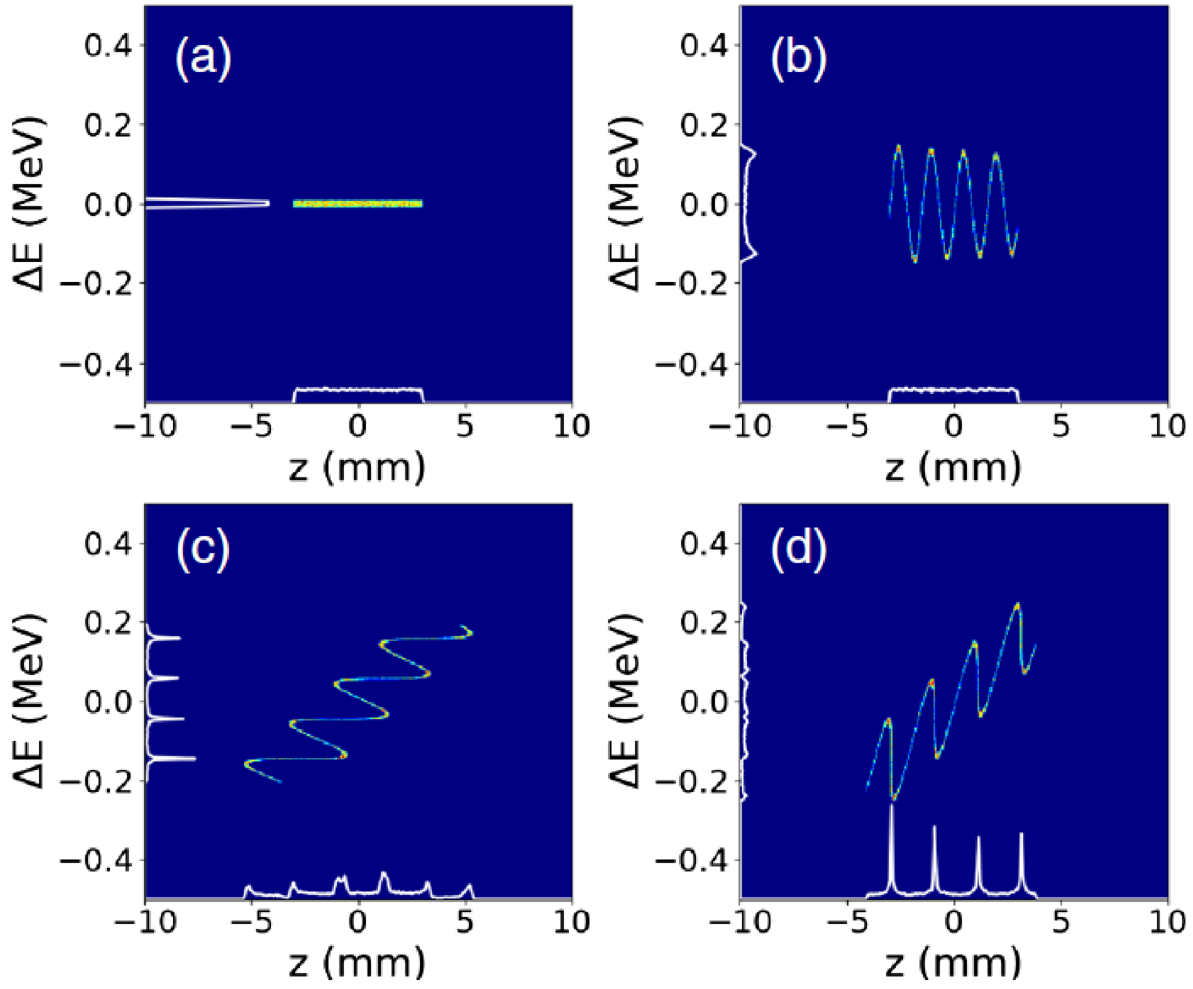

(a) The beam's initial phase space. (b) The phase space after a modulator. The final phase space after a double-EEX beamline having (c) spectral or (d) temporal bunching. From Seok et al., 2021.

Round-to-Flat + EEX

- Arbitrary 6D phase space partition
  - Round-to-flat beam transformation between the two transverse phase spaces;
  - Transverse-to-longitudinal EEX between any transverses phase space and the longitudinal phase space.

https://arxiv.org/abs/2205.03736

DAMPING RING FREE INJECTOR FOR FUTURE LINEAR COLLIDERS

TIANZHE XU, PHILIPPE PIOT

(COLLABORATIONS W/ MASAO KURIKI, JOHN
+ DISCUSSION W/ ZAK LIPTAK (HU) AND ELIANA GIANFELICE-WENDT (FNAL)]

OCT. 28TH, 2022
AWASci

DAMPING RINGS

What is damping

- Phase-space cooling is possible: Dissipative force (radiation) + restoring energy along one direction but takes time
- Storage rings naturally implement such a cooling technique via synchrotron radiation (**SR**)
- Damping ring (**DR**) are storage ring optimized to cool the beam (e.g. radiation may be produced using undulator instead of just relying on bending magnets)
- Most (all?) of the linear colliders include a DR for ILC is it 6-km complex circumference!

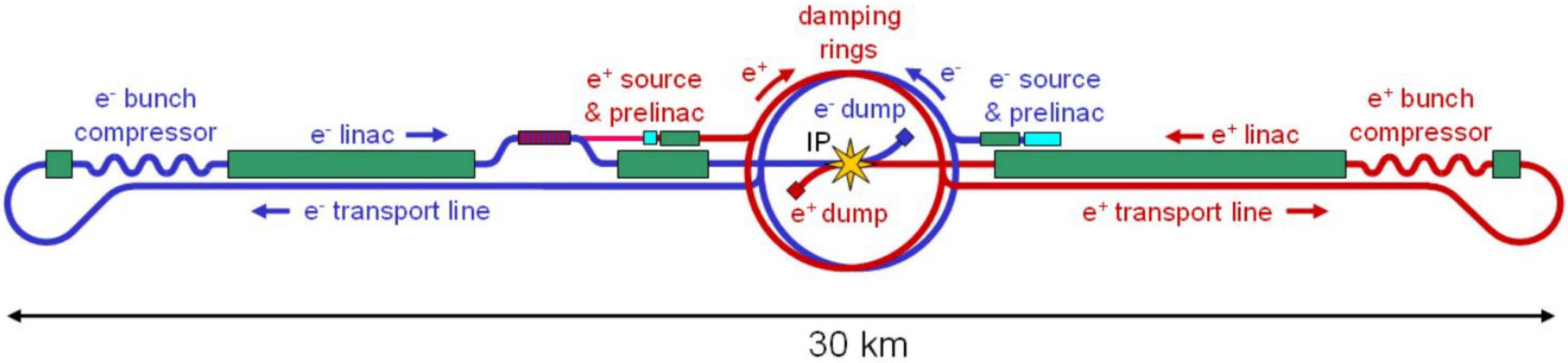

WHY DO WE NEED A DR? CAN WE DO WITHOUT IT?

Producing low vertical emittances

- Luminosity for a flat beam

power

bunch length

$$\mathcal{L} \propto \frac{P_b}{E_b} \frac{1}{\sigma_z^{1/2} \sigma_y^*}$$

power

vertical size

- The DR is needed to produced the required emittance partition in the transverse 4D plane (x,x',y,y')

	ILC	CLIC	RF gun
Reference	[7]	[8]	[5]
Charge Q (nC)	3.2	0.83	2
Energy E_b (GeV)	250	380	24×10^{-3}
ε_x (µm)	10	0.9	1.3
ε_y (nm)	35	20	1.3×10^3
σ_z (mm)	0.3	0.07	2.31
σ_δ (%)	0.19	0.35	~ 0.1
ε_z (m)	0.27	0.18	$\sim 1.1 \times 10^{-4}$
$\mathcal{B}_6$ (pC.µm^{-3})	3.4×10^{-2}	0.25	~ 11

- **Comparing 6D brightness show that the DR-beam brightness is comparable to state-of-the-art photoinjectors**

bunch charge

emittances

$$\mathcal{B}_6 = \frac{Q}{\varepsilon_x \varepsilon_y \varepsilon_z}$$

CAN WE PRODUCE THE RIGHT EMITTANCE PARTITION

Emittance repartitioning and emittance exchange

- Repartition the phase space in a controllable fashion: flat beam generation (RFBT)
- Exchange horizontal with longitudinal phase space: emittance exchange (EEX)
- The concept is not new:
  - Proposed for FEL to mitigate mu-bunching instability
  - RFBT was first invented for linear-collider application

$$(\tilde{\varepsilon}_x, \tilde{\varepsilon}_y, \tilde{\varepsilon}_z) = \begin{cases} (\tilde{\varepsilon}_m, \tilde{\varepsilon}_m, \tilde{\varepsilon}_z) \\ (2\tilde{\mathcal{L}}, \tilde{\varepsilon}_u{}^2/2\tilde{\mathcal{L}}, \tilde{\varepsilon}_z) \\ (\tilde{\varepsilon}_z, \tilde{\varepsilon}_u{}^2/2\tilde{\mathcal{L}}, 2\tilde{\mathcal{L}}) \end{cases}$$

Transverse-to-longitudinal emittance exchange to improve performance of high-gain free-electron lasers

P. Emma, Z. Huang, K.-J. Kim, and P. Piot
Phys. Rev. ST Accel. Beams **9**, 100702 – Published 25 October 2006

20 pC

Beam parameters	Value	Units
Before flat-beam transformation		
Transverse (coupled) projected x and y emittances	4.96	μm
Intrinsic transverse x and y emittances	0.23	μm
Longitudinal emittance	0.071	μm
Kinetic energy	215.4	MeV
After round-to-flat-beam transformation		
Emittance $\gamma\varepsilon_x$	9.9	μm
Emittance $\gamma\varepsilon_y$	0.0054	μm
Longitudinal emittance	0.080	μm
$\gamma(\varepsilon_x\varepsilon_y)^{1/2}$	0.23	μm

A low emittance, flat-beam electron source for linear colliders

R. Brinkmann, Y. Derbenev, and K. Flöttmann
Phys. Rev. ST Accel. Beams **4**, 053501 – Published 18 May 2001

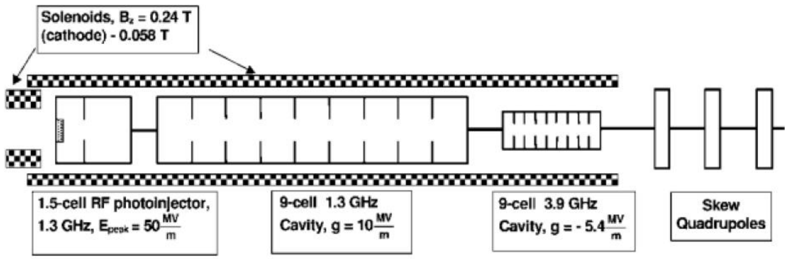

0.8 nC

Laser pulse flat top	100 ps
Bunch charge	0.8 nC
rms radius at cathode	0.26 mm
Solenoid field at cathode	0.24 T
rf gun peak electric field	50 MV/m
Booster cavity accelerating voltage	10 MV
Third harmonic cavity decelerating voltage	1.8 MV
Final beam momentum	14.2 MeV/c
rms bunch length	8 mm
Relative energy spread	0.2%
Transverse emittance	0.5 mm mrad
Estimated thermal emittance	<0.15 mm mrad

OUR APPROACH

Producing low vertical emittances

- Limitation of RFBT alone:
  - RFBT along could not produce the proper 4Demittance at the nominal ILC charge (3.2 nC).
  - Could produce a proper 4D emittance at Q=0.8 pC, (w/ a 100-ps bunch)
- Proposed concept:
  - Produced a magnetized 3.2 -nC bunch
  - Generate the required vertical emittance
  - Optimize the longitudinal emittance (via laser shaping for 3D ellipsoidal bunch formation)
  - Exchange the longitudinal and horizontal emittances

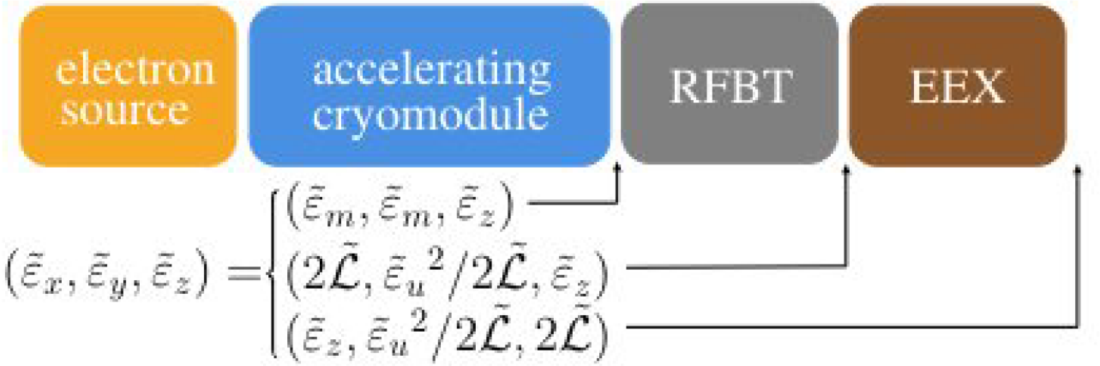

quantify the canonical angular momentum

$$\tilde{\mathcal{L}} = \frac{eB_c}{2m_e c}\sigma_c^2$$

Laser size on photocathode

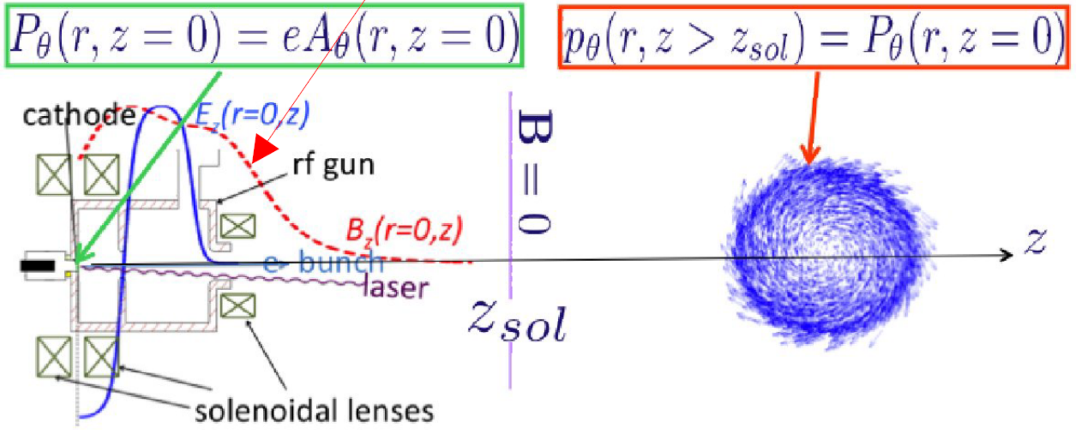

OPTIMIZING THE PHASE-SPACE OF A MAGNETIZED BEAM

Low 4D emittance + low longitudinal emittance

- Photoinjector includes
  - Shaped laser pulse
  - 1.3 GHz AWA RF-gun
  - five 1.3-GHz ILC-like cavity
- Targeting low transverse emittance results in long bunches (5-mm) → RF curvature:

$$\Delta V(\zeta) = eV_0[\cos(k\zeta + \phi) - \cos(\phi)]] \sim \zeta^2$$

- This is corrected by adding a third harmonic cavity (HCAV) decelerating the beam.

total beam energy	E_b	151	MeV
longitudinal emittance	ε_z	11.78	µm
transverse eigen-emittance (smaller)	ε_-	6.84	nm
transverse eigen-emittance (larger)	ε_+	493.4	µm
transverse uncorrelated emittance	ε_u	1.85	µm
magnetization	$\mathcal{L}$	246.7	µm

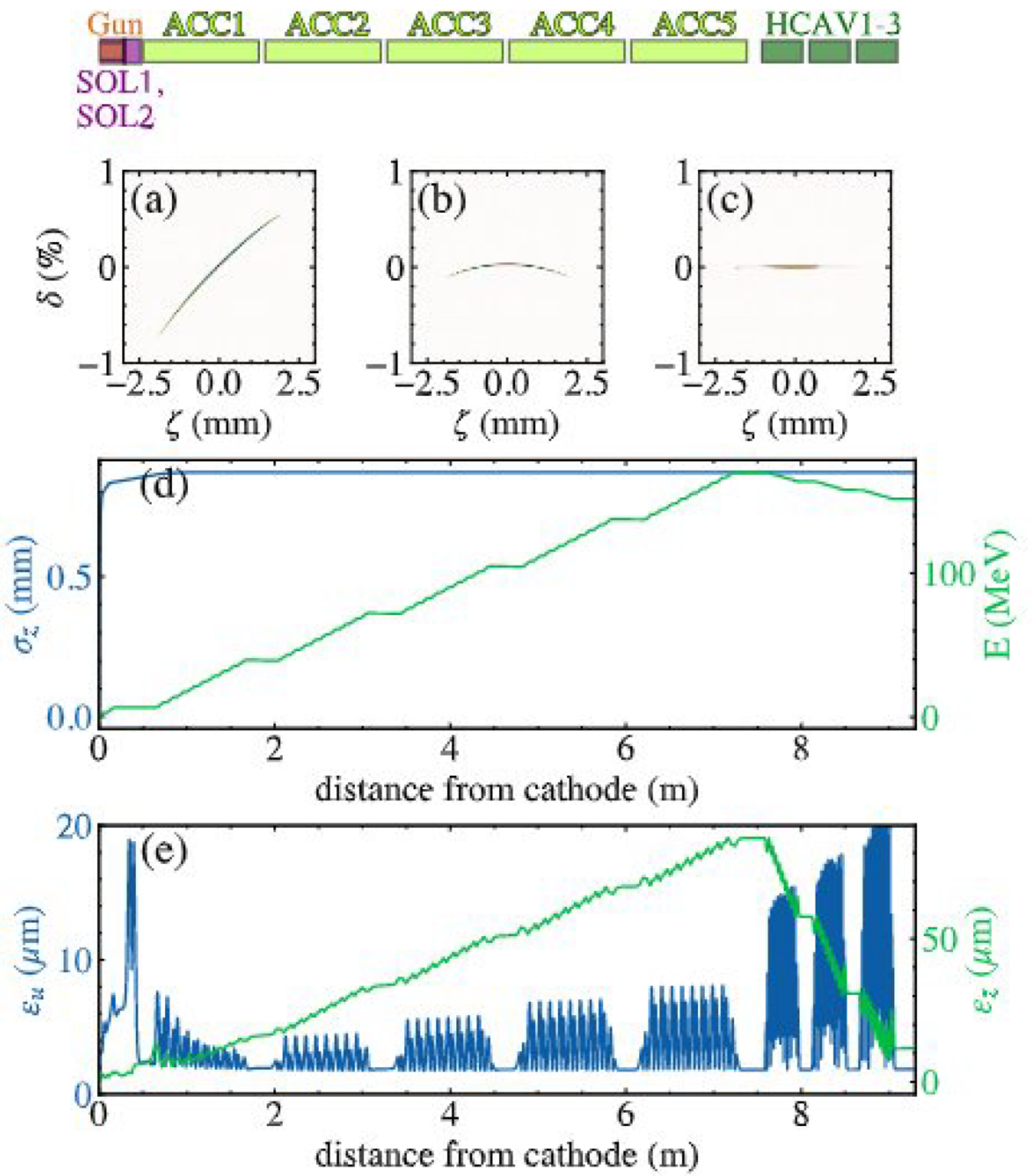

DECOUPLING & EXCHANGING

RFBT +EEX

- RFBT:
  - three skew quadrupole magnets (as at AWA)
- EEX:
  - Based on 3.9-GHz SRF cavity
  - dogleg-like configuration (B1,2,3,4)
  - accelerating cavity to compensate for thick lens aberration in deflecting cavity HCAV4-5
  - Second-order correction (sextupole magnets Si)

parameter	value	unit
skew quadrupole magnet SQ1	$k_1 = 3.71$	m^{-1}
skew quadrupole magnet SQ2	$k_1 = -7.08$	m^{-1}
skew quadrupole magnet SQ3	$k_1 = 15.76$	m^{-1}
sextupole magnet S1	$k_2 = -15.67$	m^{-2}
sextupole magnet S2	$k_2 = -1.08$	m^{-2}
sextupole magnet S3	$k_2 = -0.03$	m^{-2}
doglegs dispersion η	-1.67	m
TDC section kick strength κ	6	m^{-1}
dipole magnet B1-B4 angles	2	deg
TDC1 deflecting voltage	3.72	MV
TDC2 deflecting voltage	3.72	MV
TDC3 deflecting voltage	3.66	MV
HCAV4 accelerating voltage	5.81	MV
HCAV5 accelerating voltage	5.91	MV

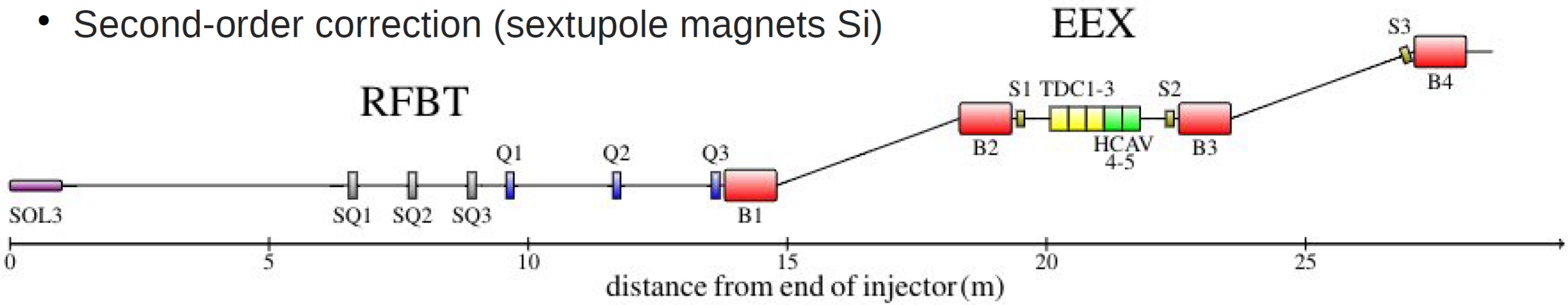

FINAL RESULTS

Emittance partition adequate for ILC

- Eigen emittances

ε_-	6.84	nm
ε_+	493.4	μm

- After RFBT:

$$(\varepsilon_{x,f}, \varepsilon_{y,f}, \varepsilon_{z,f}) = (493.40, 7.17 \times 10^{-3}, 11.82)\ \mu\text{m}$$

- After EEX:

$$(\varepsilon_{x,e}, \varepsilon_{y,e}, \varepsilon_{z,e}) = (25.47, 7.26 \times 10^{-3}, 546.34)\ \mu\text{m}$$

$$(\tilde{\varepsilon}_x, \tilde{\varepsilon}_y, \tilde{\varepsilon}_z) = \begin{cases} (\tilde{\varepsilon}_m, \tilde{\varepsilon}_m, \tilde{\varepsilon}_z) \\ (2\tilde{\mathcal{L}}, \tilde{\varepsilon}_u{}^2/2\tilde{\mathcal{L}}, \tilde{\varepsilon}_z) \\ (\tilde{\varepsilon}_z, \tilde{\varepsilon}_u{}^2/2\tilde{\mathcal{L}}, 2\tilde{\mathcal{L}}) \end{cases}$$

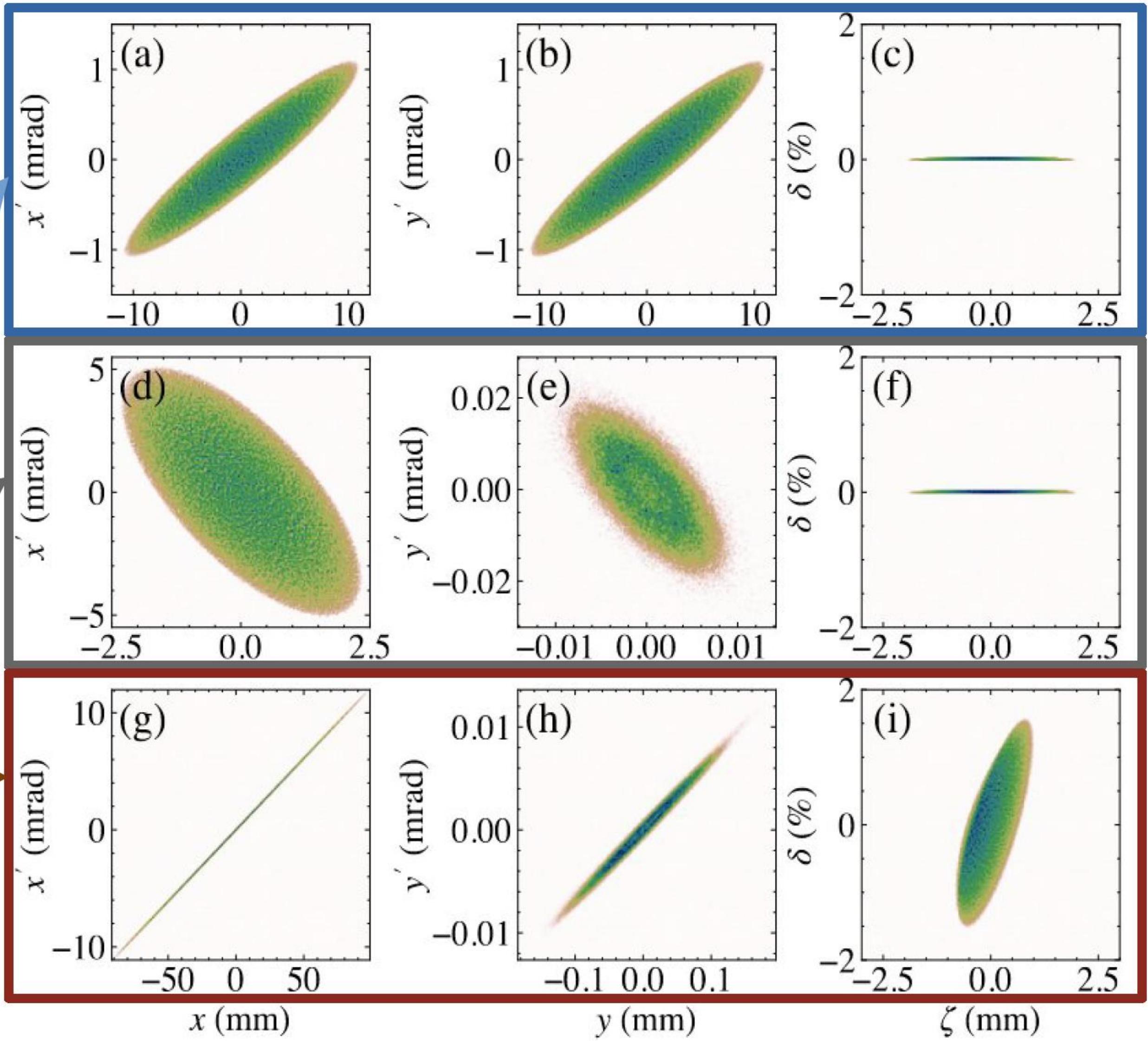

SENSITIVITY TO IMPERFECTIONS

RF jitter + laser shaping

- Impact of laser shaping was explored; sensitive to the non-ellipsoidal character

$$\left|\frac{x^2}{a_x^2}+\frac{y^2}{a_y^2}\right|^{\frac{\nu_\perp}{2}}+\left|\frac{t}{a_t}\right|^{\nu_t}=1$$

Lamé oval superellipsoid

- Impact of jitter using LCLS-II requirements for phase and amplitude stability show minimal effects

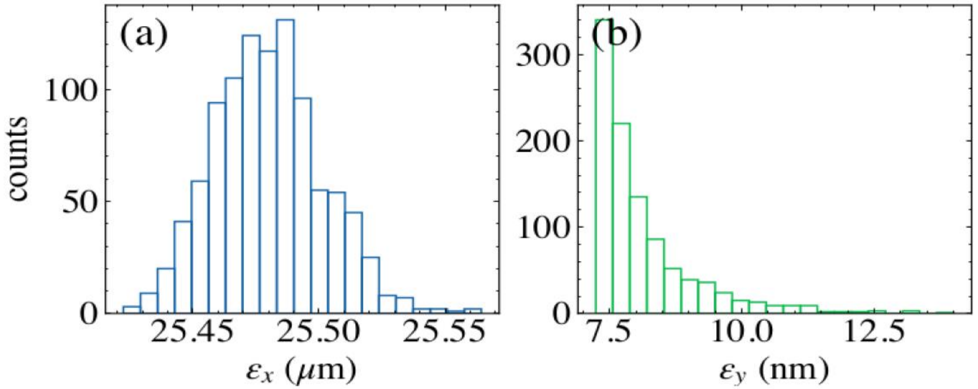

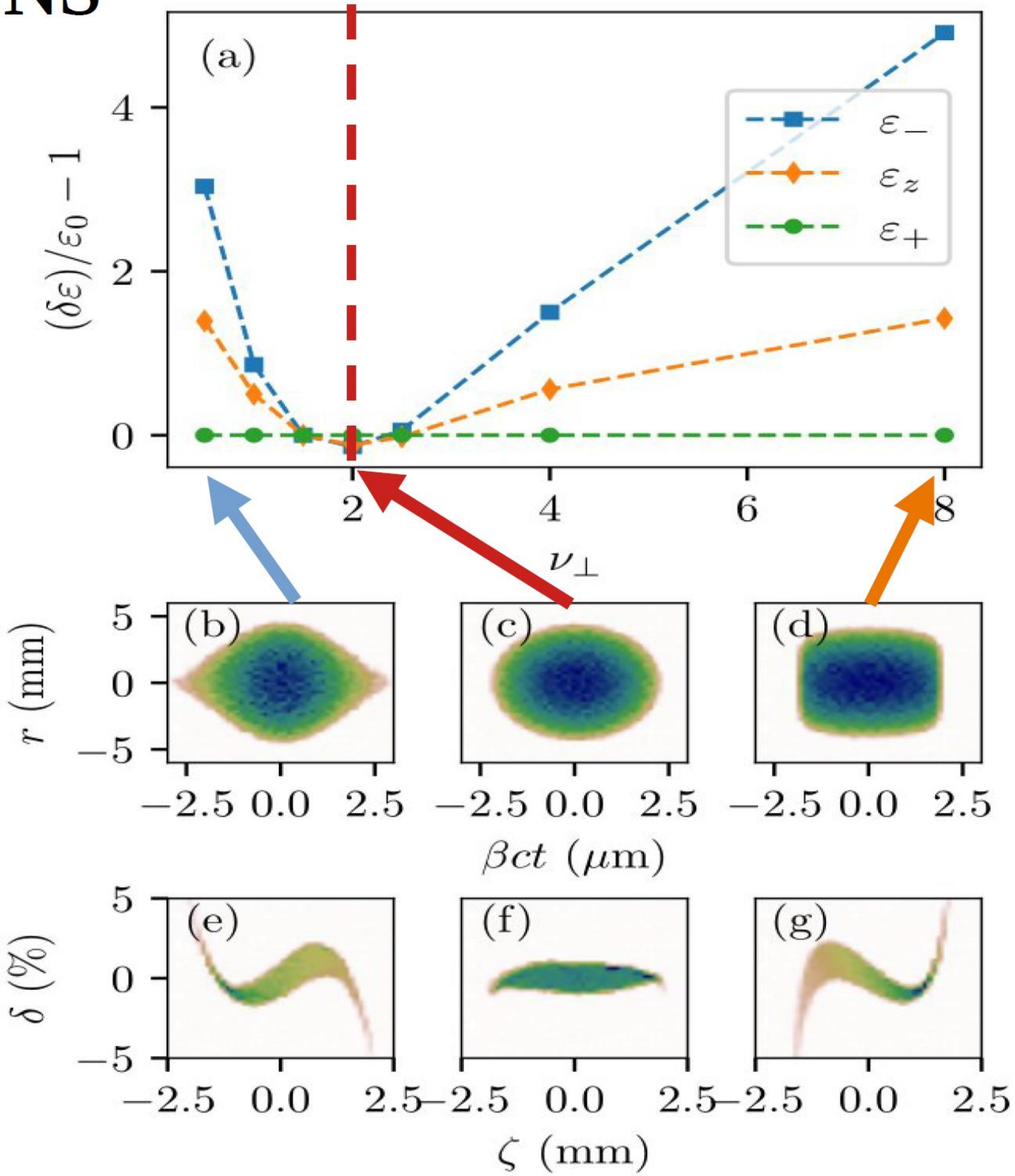

FINAL REMARKS

And open challenges…

- Design study very promising: replace a DR with a 50-m injector
- Smaller final longitudinal emittance could be beneficial (x10 shorter bunch than in ILC)
- But a lot of work:
  - RF gun are not compatible with current spin-polarized cathode technology (GaAs survives for a few RF shots)
  - The work was done for electron. Producing low 4D emittance positron beams is difficult with traditional target based methods
    - Positron trap looks appealing they inherently produced magnetized beam with magnetization comparable to the one use in our study [discussion w. S. Gessner]
    - But their current operation frequency is very low due to accumulation time

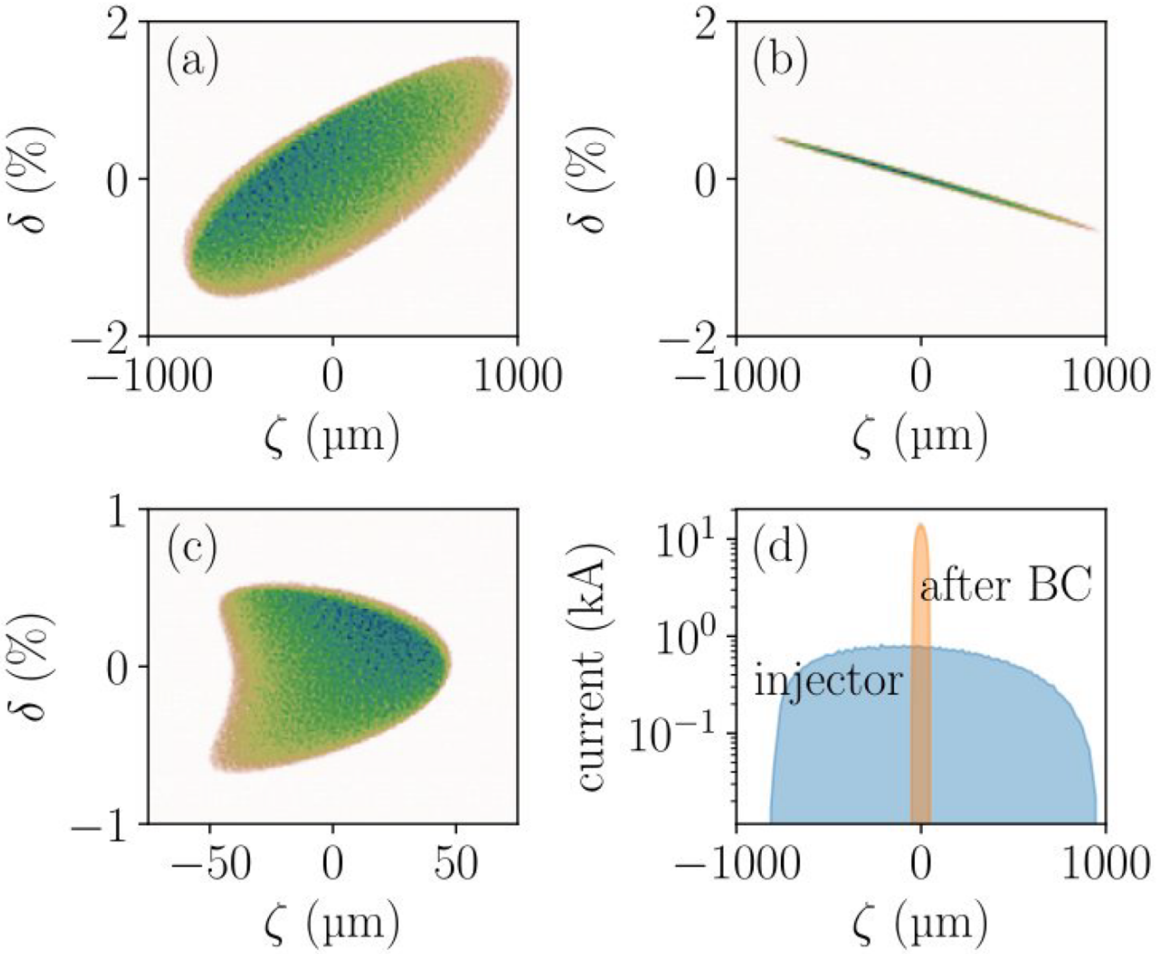

Summary

- The contents discussed in this tutorial follows the review paper: "Bunch Shaping in Electron Linac Accelerators," by G. Ha, K-J. Kim. P. Piot, J. G. Power and Y. Sun, REVIEWS OF MODERN PHYSICS, VOLUME 94, APRIL–JUNE 2022. More techniques and references on beam shaping can be found in the paper.
- Together with "Beam by design: Laser manipulation of electrons in modern accelerators," Rev. Mod. Phys. 86, 897–941 by E. Hemsing, G. Stupakov, D. Xiang, and A. Zholents, 2014, a path to finer control over the beam's phase-space distribution beyond the ensemble-averaged techniques can be derived.
- Further development of phase-space tailoring methods will ultimately aim to provide full six-dimensional control of the phase-space distributions, possibly enabling the design of a tailored beam at the single particle level.